Spring 2019

# Expendable 3D Printed Rescue Drone

Matthew Chapman
mgc13@zips.uakron.edu

Nathan Knutty
*The University of Akron*, nkk5@zips.uakron.edu

Matthew Chapman
*The University of Akron*, cjb165@zips.uakron.edu

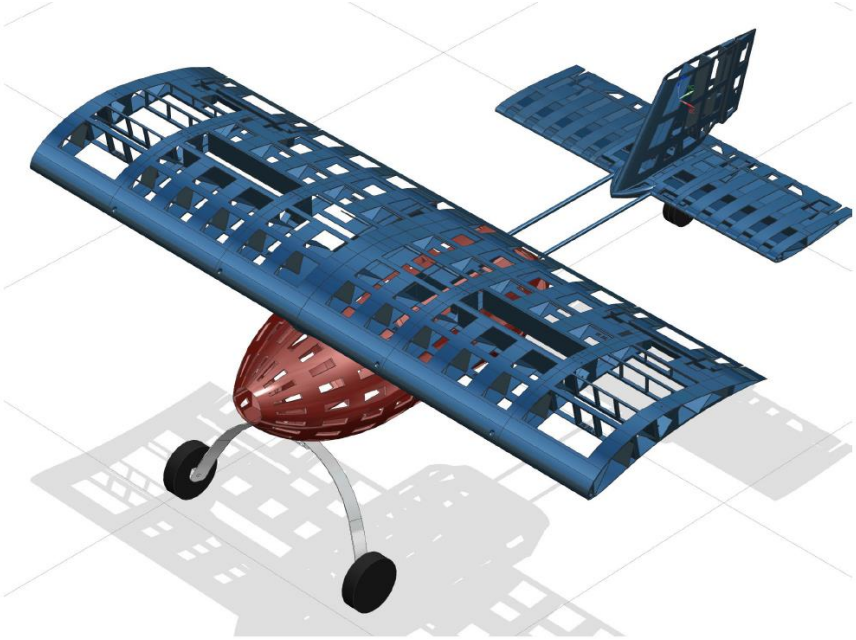

# Expendable 3D Printed Smart Rescue Drone
Senior Design Project

1 April 2019 AD

Cameron Barr
Matthew Chapman
Nathan Knutty

**Executive Summary**
This report details the design process of a fixed wing rescue drone requested by Discovery Lab Global and executed by students of the University of Akron College of Engineering. The original proposal stipulated the creation of a 3D printed drone capable of carrying a payload of at least 1.5 pounds over a period of time not to be shorter than 20 minutes.

The design process began with aerospace research and concept sketches. By using a morphological chart and weighted decision matrix, it was decided that the aircraft would be a fixed, straight, untapered, high wing aircraft with an electrical motor, moderate aspect ratio, and no anhedral. These design choices were made in order to maximize stability and improve the ease of manufacturing.

A MATLAB program was written to solve equations, as performing the analysis by hand became cumbersome due to the frequently changing values. Every decision that was made caused a previously determined value to change, therefore requiring the mathematical analyses to be completed again. From these calculations, the design team was able to determine the dimensions of each component in order to keep the aircraft functional.

From the computational, theoretical analyses performed on the aircraft and the experiments conducted in taxi tests, it was determined that the design met and surpassed all of the project requirements.

**Acknowledgements**
This team would like to thank the North Canton Hawks Radio Control club for their generosity in providing an experienced drone pilot for test flights. Their piloting expertise is greatly appreciated.

This team of three students, in conjunction with Luisa Echeverry, Isaiah Kaiser, Nathan Nicholas, and George Rusinko, completed a joint effort for the final project in Introduction to Robotics and Control to design and develop the Autonomous Robotic Safety System. Their assistance on this project is greatly appreciated.

The team also extends special thanks to advisors Dr. Rob Williams (Discovery Lab Global) and Dr. Shao Wang (University of Akron), in addition to readers Dr. Daniel Deckler (University of Akron) and Dr. S. Graham Kelly (University of Akron).

Furthermore, the team would like to recognize Discovery Lab Global for making available a 3D printer to the team and the University of Akron Department of Mechanical Engineering for printing various components of the aircraft.

**Table of Contents**

## Introduction

### Background

While many inhabited areas are easily accessible in emergency scenarios, rescue workers frequently cannot reach individuals in distress within a desirable timeframe. Often derelict hikers, climbers, and other adventurers must waste valuable time awaiting rescue. This wait can last hours or even days, and can exacerbate the individuals' already poor circumstances, even leading to their deaths.

To combat this dilemma, this team has designed a 3D printed, expendable drone capable of carrying a payload of emergency supplies to people in distress who are in remote areas. The initial requirements provided by Discovery Lab Global called for an aircraft capable of carrying at least 1.5 pounds of payload for a duration of 20 minutes. The aircraft will also serve as a testbed for Artificial Intelligence research in the future.

### Principles of Operation

In order to provide assistance to rescuees, the aft portion of the fuselage features a cargo bay that can contain many supply items such as water bottles, first aid kits, etc. To reach such isolated targets, the aircraft was designed to be able to takeoff from most surfaces. Once in the air, the pilot levels off and reduces power to the motor. This allows the aircraft to maximize its range while still arriving in a reasonable amount of time. If the rescuees require more immediate attention, the aircraft can fly at maximum speed to the target; however, flying at high speeds is less fuel efficient and will decrease the range of the aircraft. After the aircraft has arrived at the target, it will go into a steep dive and deploy a parachute. The purpose of the dive is twofold: it assures ample airspeed for the parachute to properly open while helping keep the aircraft headed directly toward the target. Once the aircraft has landed, the target individuals can remove the supplies from the cargo bay and dispose of the aircraft, as it is intended to be expendable.

The aircraft also features an advanced Autonomous Robotic Safety System (ARSS). If certain flight conditions have occurred that may threaten the safety of those near the aircraft, it will autonomously initiate an emergency landing by launching the parachute. These flight conditions are detailed below.

1. The battery is nearly dead
2. The aircraft has lost communication with the pilot
3. The aircraft has engaged in a "high G" maneuver that could destroy the aircraft in midair
4. The aircraft has caught on fire

This addition to the aircraft was designed for the purpose of improving its safety. Because the aircraft is capable of being operated by novice pilots and beyond the line of sight, it was determined that additional safety measures would augment the overall airworthiness of the aircraft.

Product Definition

The subject of this design project is a fixed wing electric aircraft that features a straight, untapered wing. The original project posting made by Discovery Lab Global presented the following design constraints:

1. Capable of carrying a payload of no less than 1.5 pounds
2. Capable of flying for no less than 20 minutes
3. Manufacturable via 3D printing on a small, inexpensive device
4. Capable of delivering a payload with reasonable GPS accuracy
5. Capable of being used as a testbed for AI technology
6. Easily replicable

As a result of the above constraints, the aircraft is designed to be primarily made of PLA plastic. Furthermore, the physical structure of the aircraft was designed to be conducive to the 3D printing process. The final product delivered to Discovery Lab Global is a Remote Controlled (RC), 3D printed aircraft equipped to deliver emergency supplies to individuals in distress in remote locations.

## Conceptual Design

Aircraft

The design criteria immediately forced several design decisions in a certain direction. For example, many of the aerodynamic parameters were chosen to support a mission type that would require high stability. In Figure 1 a Morphological Chart can be seen from one of the project notebooks.

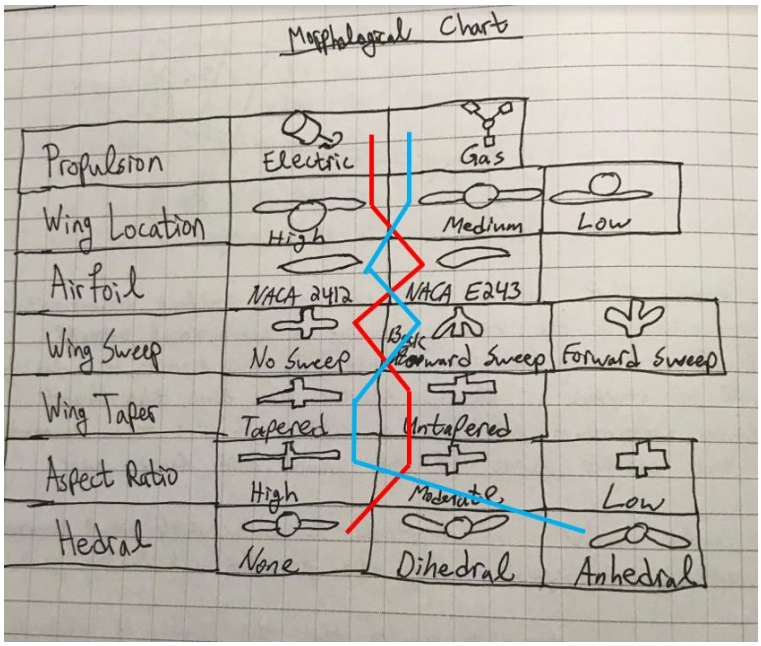


*Figure 1*. Morphological Chart from Matthew Chapman's project notebook.

The most pressing decision to be made was the propulsion. It was determined that the aircraft should be powered by a brushless DC electric motor because of the large availability of these motors and the reduced risk of carrying non-flammable fuel. Next, the team chose for the aircraft to feature a high wing position. This parameter is typically varied on aircraft in order to manipulate the aircraft's stability, as the wing position determines the point of support for the aircraft. When flying, the aircraft is supported by the wings, which connect to the fuselage at the wing root. Fighter planes that must execute tight maneuvers typically have low wings, while cargo aircraft typically have higher wing positions in order to keep them stable. Stability was a large concern for the drone, as 30 percent of the aircraft's total weight can be its payload. These cargo items can be placed in the aircraft in numerous configurations that have the potential to greatly affect the center of gravity. By placing the wings high, it can be ensured that the center of gravity will always be below the point of support.

Two airfoils – NACA 2412 and E423 – were considered for this project. Because of the requirement for the drone to be 3D printed, it was assumed that the drone would have a very large mass. This is due to the relatively large density of PLA plastic compared to balsa, Styrofoam, and other light materials commonly used for RC aircraft. To increase lift and decrease the takeoff speed, NACA E423 was selected because it had a very large coefficient of lift (see Figure 2). This selection was made with priority given to high lift at low speeds, despite the possible consequence of large amounts of drag at high speeds. As a rescue aircraft, takeoff and low speed performance were deemed more important than high speed flight performance.

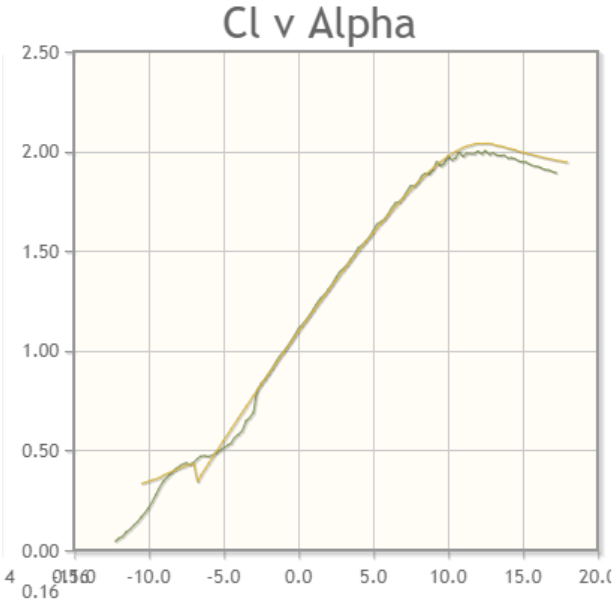


*Figure 2*. Coefficient of Lift vs. Angle of Attack for E423 at Re = 200,000 and Re = 1,000,000. Adapted from AirfoilTools.com.

Wing sweep was another design consideration studied for this project. Wing sweep is primarily utilized on supersonic and transonic aircraft in order to delay shock waves and the drag induced thereof. At low subsonic speeds, swept wings cause spanwise flow, an aerodynamic condition in which air hitting the leading edge of a wing travels around the wing rather than over or under the wing. Not only does this reduce lift, but it also increases drag. For this reason, it was immediately determined that the aircraft would feature a straight wing.

Next a tapered wing was considered. A tapered wing is a wing in which the chord varies with respect to the distance traveled down the span. Such wings increase the aspect ratio of an aircraft while minimizing the bending moment caused by the static load of the weight of the wing, making it ideal for this aircraft. Despite this, tapered wings would make each wing part unique and, therefore, not interchangeable. This would make part replacements difficult and would require substantially more spare parts to be kept on hand, so the team decided to design the wing to be untapered.

The aspect ratio of an aircraft is an engineering parameter utilized to indicate the ratio of the length of a wing's span to the length of its chord. Large aspect ratios lead to higher lift to drag ratios, which improve aircraft fuel economy; however, there are many disadvantages as well. Among these are reduced maneuverability caused by the increased moment of inertia and the increased bending moment caused by lift acting on the wing. Because PLA is not a particularly strong material, the concern arose that a high-acceleration maneuver could threaten to rip the wings off the fuselage, failing due to excessive bending moment. So, because the fuel economy of a high aspect ratio and the maneuverability and strength of a low aspect ratio were preferred, the design was restricted to a moderate aspect ratio. This was also accompanied by the increased benefit of allowing the design team to curtail the wing dimensions to large values that would maximize lift.

Finally, the team considered another facet of the design: anhedral, which is the sloping of an aircraft's wings down toward the end of the span. When aircraft with high or medium wing positions are too stable, aircraft designers often employ anhedral to the wings to reduce stability. Because the mission type does not require high maneuverability, the drone was designed with no anhedral, thus maximizing the stability of the aircraft.

From the Morphological Chart (Figure 1), two concepts were created and compared via an Objective Tree (see Figure 3). Within the tree, percentage values were assigned in order to evaluate the need for each objective.

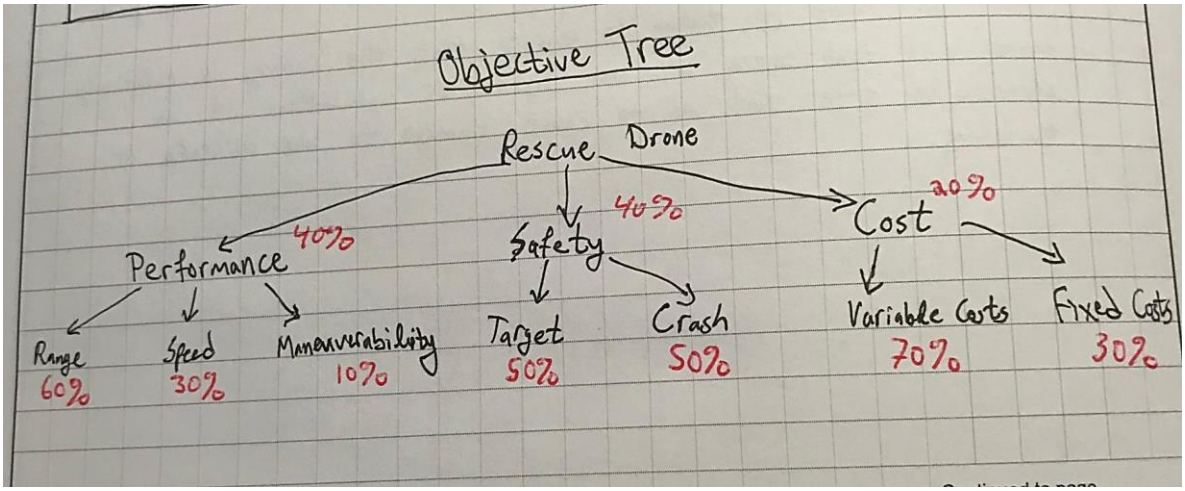


*Figure 3*. Objective Tree for drone design from Matthew Chapman's project notebook.

Once the Objective Tree was completed, both concepts were compared in a weighted decision matrix (see Appendix A) whose results can be seen in Figure 4.

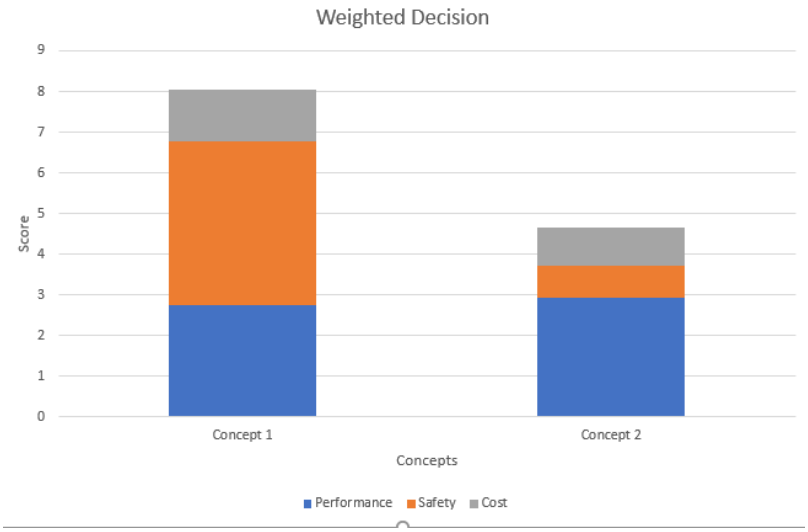


*Figure 4*. Weighted Decision Matrix Results.

Although Concept Two had a slight advantage in terms of performance, Concept One was clearly and decisively the best design for the project. Concept Two's complex parts and lack of an Autonomous Robotic Safety System caused it to be too expensive and unsafe. The remaining design, Concept One, can be seen in Figure 5 as a preliminary sketch.

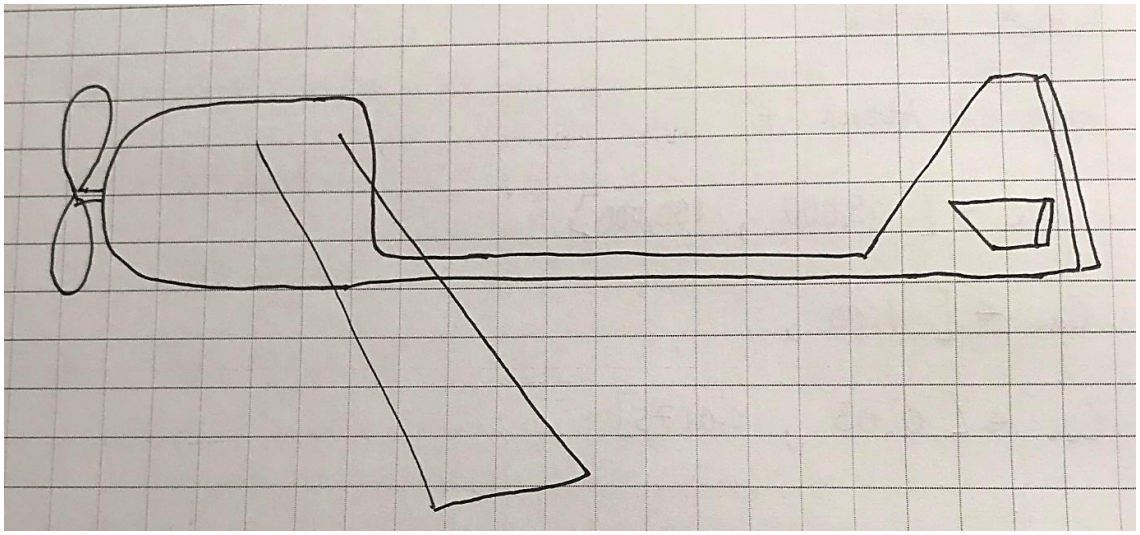

*Figure 5*. Sketch of Conceptual Design (Concept 1) from Matthew Chapman's project notebook.

Autonomous Robotic Safety System

Preliminary discussions of potential failure modes led to the idea of incorporating a safety system that would override novice pilots, design flaws, and poor artificial intelligence piloting software. For this system, four main potential failure modes were chosen: low battery, communication loss, over maneuvering, and fire onboard. An Arduino product was added to Concept One as a result.

**Embodiment Design**

Aircraft

To fulfill its mission, the drone has many components. A cross sectional diagram of the basic design can be seen below in Figure 6. As indicated in the image, many of the components were situated based on necessity; for example, the engine had to be positioned forward in order to drive the propeller. Other items such as the battery were positioned in order to manipulate the aircraft's center of gravity, which was intended to be one third of the distance aft along the wing chord length to maximize in-flight stability. Preliminary analysis indicated that the center of gravity would be too far aft, so heavier components were moved forward. The remaining components were simply positioned where space was available.


*Figure 6*. Cross sectional view of Embodiment Design

The material constraints of this product limited the design team's options for interfaces. Because of these limitations, unique interlocking mating interfaces were designed (see Figure 7). When the interfaces themselves were insufficient to bear the necessary load, M5 screws were introduced. The implementation of non-permanent fasteners such as these screws allowed optimal load management while also minimizing manufacturing difficulty. The wings (seen in Figure 7) are the components of the aircraft that are subjected to the most load. Because of this, great care was taken to ensure that the wing part mates were strong enough to sustain even the most brutal of maneuvers. This was accomplished with reinforcing screws adjoining each part to the next contiguous part.

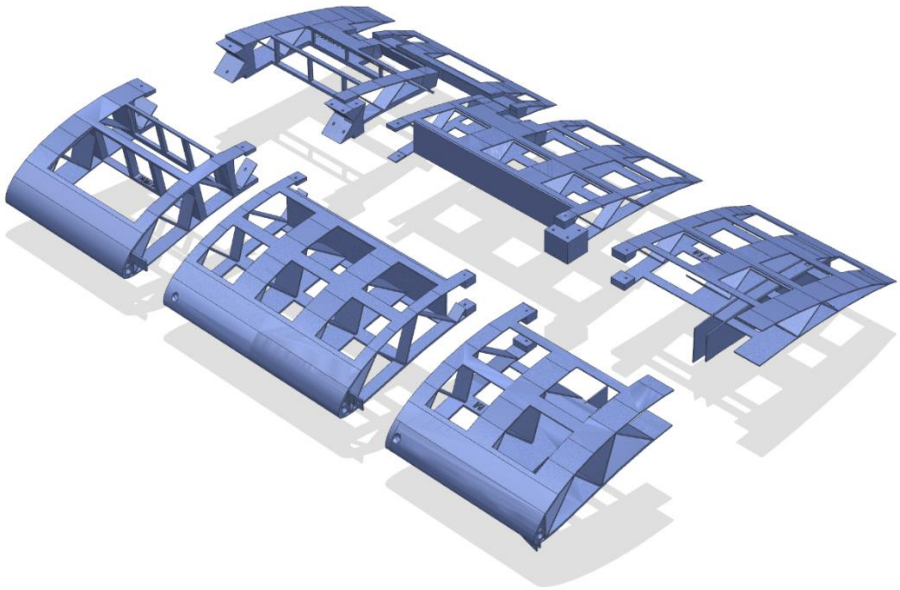

*Figure 7*. Wing mating interface.

Embodiment Design Rules and Principles were utilized to enhance the drone's overall design. In order to increase the clarity of function for the pilot, the controls system was setup in a manner typical of RC aircraft. This allowed experienced pilots to easily operate the aircraft. The drone was also designed to embody simplicity. Because of the constraint requiring that the aircraft be 3D printed, manufacturing times became very large. To combat this, structures were designed to be as simple as possible. For the entirety of the project, no design parameter was more important to the design team as safety. Because of the very nature of the drone being a rescue device, safety was intrinsically necessary to the mission. One particular safety feature is the ESC low battery power management. This option cuts all power to the engine once the battery is nearly depleted. As a result, the aircraft is forced into glider mode, a flight condition in which only the control surfaces are operable. This option augments safety by reserving what little power is left so the pilot can safely land the aircraft. Other landing and safety options are discussed in the Autonomous Robotic Safety System Embodiment Design Section. Furthermore, the drone was designed to minimize its impact on the environment by using sustainable components and no toxic or abrasive chemicals.

The force transmission of the aircraft was simplified by placing the motor in close proximity to the propeller. Because of this, there is no need for a driveshaft. The propeller is directly mounted to the motor's shaft. Electrical components were designed to be redundant and therefore exhibit a division of task. The entire aircraft could have been controlled by an Arduino Board; however, a single electronic or programming failure could have resulted in a catastrophe. Instead, the aircraft is controlled by a dedicated receiver while the ARSS is controlled by its own Arduino Board.

Due to simplification and cost constraints, the drone was designed not to be equipped with flaps. Flaps are a control surface used by fixed wing aircraft in order to raise the static pressure on the lower surface of the wing. This results in an increase in both lift and drag, which is advantageous during landing and, to a small extent, during takeoff. Without flaps, preventing excessive speed during landing is exceptionally difficult. Because of this, the aircraft is designed to have non-retractable landing gear. The landing gear is always deployed and, therefore, always contributing additional drag to the aircraft. By both managing speed and allowing the aircraft to takeoff and land conventionally, the landing gear is one of many examples of self help in this design. As previously indicated, the aircraft was also designed for maximum stability. This was achieved via its high wing mounting position and no wing anhedral.

To ensure that all possible disasters were understood and accounted for, a Design Failure Mode and Effects Analysis (DFMEA) was completed (see Appendix B). From this, 26 unique and individual failure modes were identified amongst the 14 major components of the aircraft. For each failure mode, effects, severity, causes, and prevention were detailed. In addition to this, a

formula was derived to calculate the Danger Factor. The Danger Factor is a parameter used to determine the inherent risk of any specific failure mode and is composed of the severity of the failure mode combined with the likelihood of it occurring, then scaled to a percent-based scale. Then the extent to which the failure mode is mitigated by the ARSS was considered and utilized in the formation of a new parameter – the ARSS Danger Factor. This parameter indicates the risk associated with a given failure mode and the extent to which the ARSS mitigates that risk. In general terms, the overall risk associated with any failure mode can be indicated using the ARSS Danger Factor, as this accounts for the overall safety of the aircraft. For the DFMEA, Severity was determined by the convention set in Table 1.

*Table 1*

*Convention for Severity Assignments in the DFMEA*

| Score | Criteria |
|---|---|
| 1 | No impact to performance |
| 2 | Non-dangerous impact to performance |
| 3 | Dangerous impact to performance |
| 4 | Catastrophic failure possible |
| 5 | Catastrophic failure imminent |

Because fixed wing aircraft operate above the ground and at high rates of speed, any failure has the potential to end in disaster. This is indicated by the large number of high-severity failure modes as seen in Figure 8. Nearly half of the failure modes were predicted to result in an imminent catastrophic failure. Despite the severity, Figure 9 demonstrates that a combined 84 percent of the failure modes can be categorized as “unlikely” or “very unlikely.”

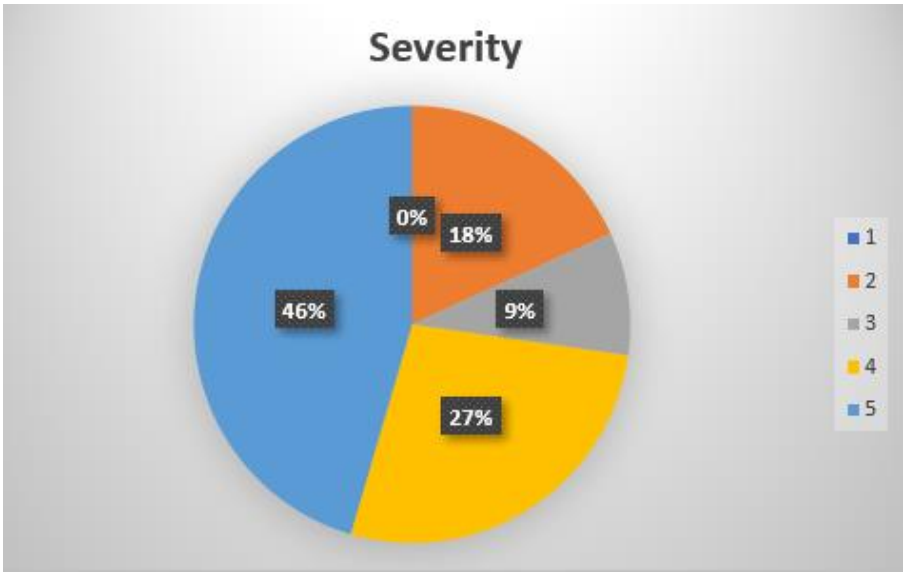


*Figure 8*. Severity of failure modes in the DFMEA.


*Figure 9*. Likelihood of failure modes in the DFMEA.

With the DFMEA data, it can be unequivocally demonstrated that the ARSS greatly improved the safety of the aircraft. Table 2 indicates the ARSS Mitigation convention used in the DFMEA. Figure 10 shows the ARSS Mitigation values for the various failure modes. As depicted in the chart, a combined 60 percent of the failure modes were “mostly mitigated” or “completely mitigated” via the introduction of the ARSS.

Table 2

*Convention for ARSS Mitigation Assignment in the DFMEA*

| Score | Criteria |
|---|---|
| 1 | No mitigation |
| 2 | Limited mitigation |
| 3 | Moderate mitigation |
| 4 | Mostly mitigated |
| 5 | Completely mitigated |

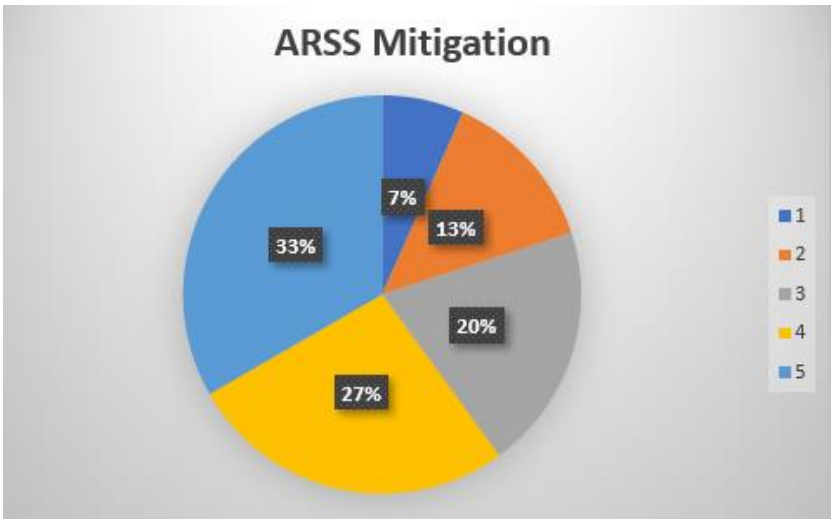


*Figure 10*. ARSS Mitigation values from the DFMEA.

Because of project constraints, the materials and manufacturing practices used were largely determined prior to beginning design work. Most of the aircraft is 3D printed, with a small number of carbon fiber rods used due to their high strength to weight ratio. PLA plastic was used as the primary printing material due to its ability to be printed on low-quality printers. Material specifications of PLA can be found in Appendix C. Printing with other materials like ABS on such printers can lead to warping and misprints. These plastics, however, have a relatively low strength to weight ratio, and so it was decided to construct the entire aircraft as a skeleton with holes in the structure (see Figure 11). Once the aircraft has been completely assembled, it is wrapped with a thin layer of plastic that acts as skin. It was also determined that no individual part could exceed 210 millimeters in any direction, as this is a common maximum dimension for most low-end 3D printers.

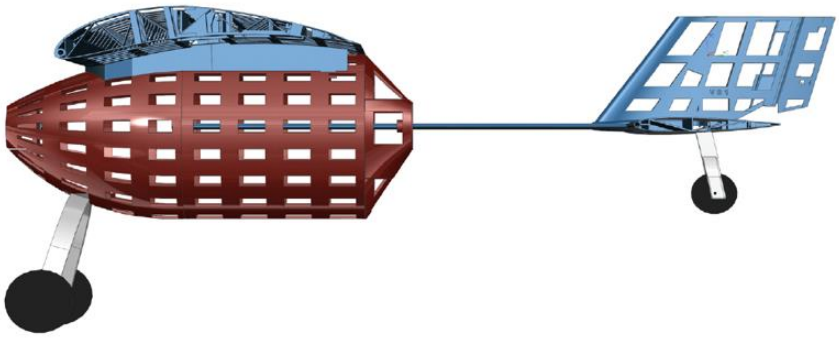

*Figure 11*. View of aircraft with holes in structure.

While designing the aircraft and making preliminary calculations, two things became very evident. The first was that all parameters of the design had to be guessed rather than known.

There was no means by which to accurately estimate the weight or coefficient of drag of the drone without knowing the full list of components and physical geometry. Second, this source of error meant that calculations would have to be run many times with varying values. That is, takeoff and flight considerations had to be made by performing analysis with many different weights, coefficients of drag, and other values. To do this, a Graphical User Interface (GUI) was created in MATLAB (see Appendix D). The general design of this MATLAB program was to list known or accepted values and then perform various analyses based on the desire of the user. A snapshot of the GUI can be seen in Figure 12 with all the analysis options. Values from this program can be seen in the Performance section of this report. All equations used in this program can be seen on the Equations pages of Matthew's project notebook in Appendix E.

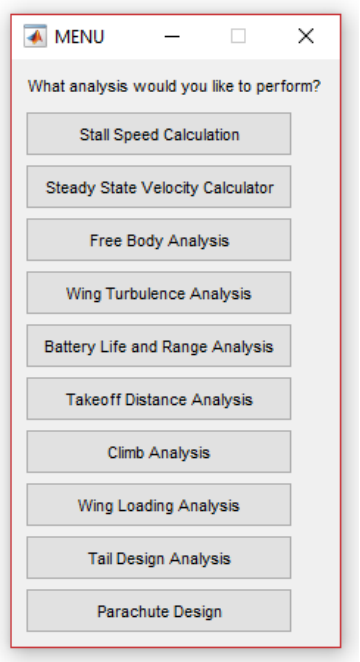


*Figure 12*. MATLAB GUI for numerical analysis.

The unusual payload and material constraints of this project incurred one performance consequence that was paramount to all others: excessive weight. When designing the aircraft, every opportunity was taken to reduce the weight of the drone; nevertheless, the weight was still projected to go in excess of 4 kilograms. To counter this, the wing surface area was increased, and the propulsion was decided to be very powerful. Ultimately, the design team settled on the T-Motor U5 KV400 (see Appendix F for OEM specifications). Equipped with the manufacturer's recommended propeller, this motor can produce up to 19.9 Newtons of force. This large thrust was deemed necessary in order to get such a heavy aircraft off the ground and up to a safe altitude quickly. The electrical architecture of the aircraft – discussed in the Detail Design section of this report – was predominantly designed around the motor due to its demanding electrical needs.

Autonomous Robotic Safety System

During the design of the aircraft, it became apparent that fixed wing aircraft, such as the subject of this study, are prone to catastrophic failures due to their need to operate at high speeds and altitudes, in contrast to ground and sea-faring vehicles. This vehicle in particular was also subject to another potential source of catastrophe - novice pilots. Because of the nature of the drone being RC, almost anyone could try to operate the aircraft, regardless of skill level. The design team eventually settled on equipping the drone with a robotic system capable of landing the aircraft even when the pilot was oblivious to or in denial of seriously dangerous flight conditions.

The Arduino Uno Board was selected as the central hub for this system due to its low cost, ease of use, and availability. The primary operation of the system was designed such that the aircraft deploys a parachute if either the pilot orders it so or if the ARSS detects dangerous flight conditions (discussed in the Introduction – Principles of Operation section of this report). From the preliminary design stages, it was decided that the parachute would either be stored in the upper portion of the fuselage or externally stored underneath the belly of the aircraft. The former was ideal for aesthetics and performance, while the latter was preferable for maximizing payload size. Furthermore, the size of parachute required was not known, so it could not be determined whether the parachute could fit inside the aircraft. In this configuration, the profile would resemble that of World War Two aircraft featuring drop fuel tanks.

**Detail Design**

Aircraft

When a fixed wing aircraft is in flight, there are four principle forces acting upon it: lift, thrust, weight, and drag. These forces can be seen schematically on the free body diagram in Figure 13. In general, it is desirable for engineers to minimize drag and weight while maximizing lift and thrust. This is intended in order to optimize the aircraft's performance while minimizing its losses and undesirable performance characteristics.

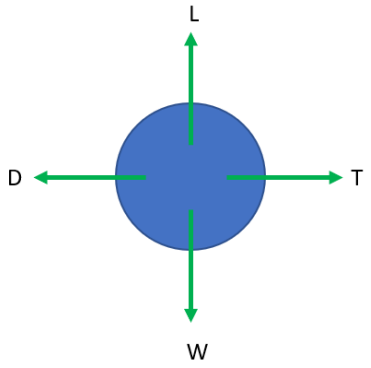


*Figure 13*. Free body diagram of the aircraft.

The free body diagram displayed in Figure 13 assumes the most trivial case that the aircraft is flying even with the horizon; that is, the angle of attack is zero. While this occurs frequently during normal flight operation, the aircraft can also pitch up and down. In this event, the free body diagram changes to resemble Figure 14. In Figure 14, the aircraft is assumed to have an arbitrarily positive angle of attack; that is, it is climbing. In this scenario, the thrust, lift, and drag change direction. The thrust is always oriented in the direction in which the aircraft is aimed. This is because the thrust is generated by the propeller, which is fixed to the front of the aircraft. It must be stated that this assumption is not valid for aircraft equipped with thrust vectoring capabilities; however, this aircraft features a fixed propeller. The lift force changes because the resulting force is generated normal to airflow over the wings. When the wings are inclined, the lift force will also rotate. Drag always acts axially to the wings, so it is also rotated. Finally, the weight force does not change because it is always directed to the center of the Earth, which has not changed. If the aircraft is descending, the values of alpha can simply be made negative.

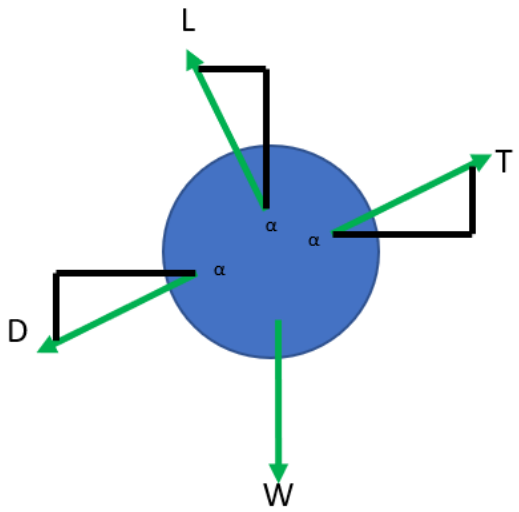


*Figure 14*. Free body diagram of the aircraft with $\alpha > 0$.

To better understand the limitations of the aircraft, an analysis was conducted of its climbing abilities. From the free body diagram seen in Figure 14, two equations were derived: one for the steady state speed in a climb and the other for the stall speed in a climb. The two equations can be seen below. For their respective derivations, see page 21 of Matthew's project notebook in Appendix G. The steady state speed is a flight parameter that indicates at which speed the aircraft will fly as time approaches infinity, assuming no changes in control occur. The stall speed is a flight parameter that indicates the minimum speed at which the aircraft can fly without the weight force becoming greater than the vertical component of the lift force.

$$v_{ss} = \sqrt{\frac{T - mg\sin\alpha}{\frac{1}{2}\rho A_a C_D}}$$

$$v_s = \sqrt{\frac{2mg\cos\alpha}{\rho A_w C_L}}$$

In order to sustain stable flight conditions and avoid stalling the aircraft, the steady state speed must always be greater than the stall speed. Figure 15 shows a MATLAB plot of the aircraft's speed versus angle of attack assuming various other parameters such as mass and area of the aircraft. From the chart, 24 degrees is the maximum sustainable angle of attack that the aircraft can achieve. This value must, however, be accompanied with a caveat. The maximum sustainable climb rate is a function of engine power, mass, geometry, and weather conditions. Because of this, it can vary greatly from one flight to another. It is therefore suggested that no pilot ever attempt to sustain an angle of attack of greater than 20 degrees. In order to maintain safe conditions, the drone should only be operated below the red dotted curve and to the left of the blue solid curve.

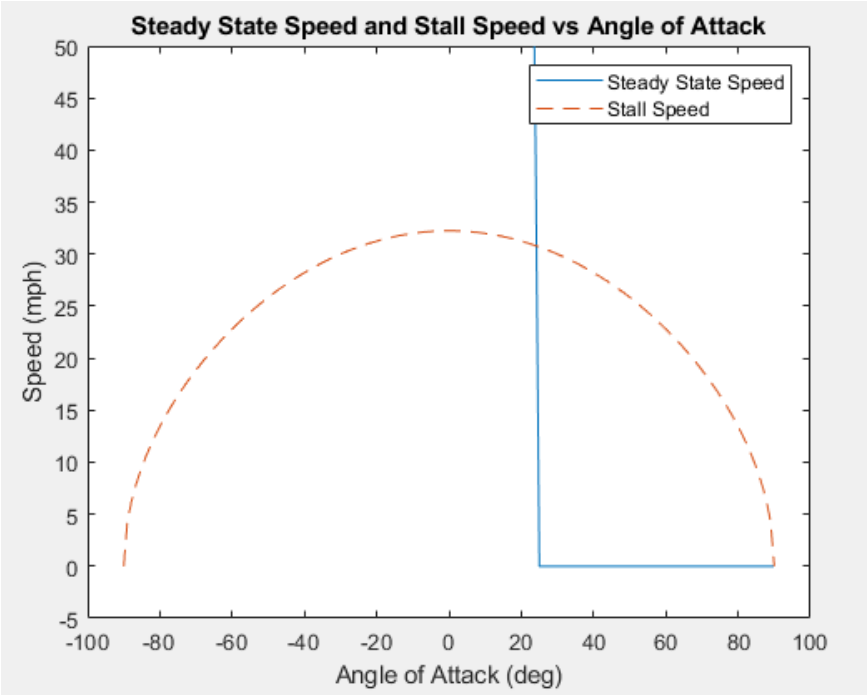


*Figure 15*. Chart of steady state speed vs. angle of attack for the aircraft.

A distinction that must be made is the difference between maximum rate of climb and maximum sustained rate of climb. The former is simply the greatest angle of attack the aircraft can assume for a small amount of time; whereas, the latter is the largest angle of attack the aircraft can

assume as time approaches infinity. Because of the difference, the aircraft certainly can climb at angles of 40, 50, and possibly even 60 degrees; however, this can only be performed for short periods of time when the initial velocity prior to the maneuver is sufficiently high.

During takeoff, the free body diagram changes once again. As seen in Figure 16, the four principle forces remain unchanged from Figure 13 where the aircraft is in level flight; however, a new force has been introduced. As the aircraft traverses down the runway, it encounters frictional loses at the landing gear. Because takeoff occurs at relatively low speeds and drag is predominantly a function of speed, the greatest source of resistance to acceleration is friction.

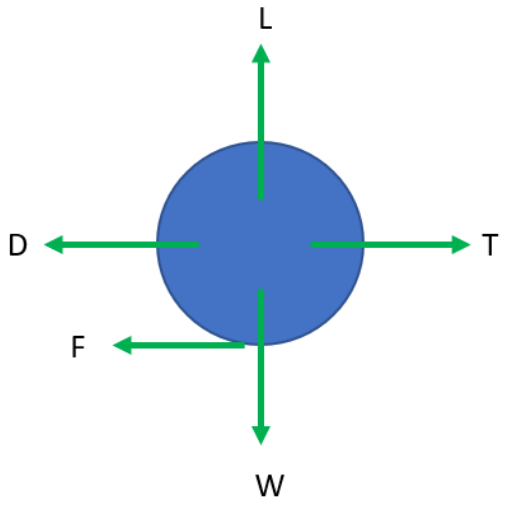


*Figure 16.* Free body diagram of the aircraft during takeoff.

From the diagram above, the takeoff distance can be calculated. To see the derivation of this equation, reference pages 19-20 of Matthew's project notebook in Appendix H.

$$x_{to} = \frac{(FS)m^2 g}{(\rho A_w C_L)\left(T - \frac{A_a C_D mg}{A_w C_L} - \mu_f mg\right)}$$

A numerical value is not calculated here because it is entirely dependent on the mass of the aircraft and the surface conditions of the runway. The former varies greatly with payload size and the latter varies with location and weather. The friction coefficient, $\mu_f$ must also be experimentally determined, which has its own associated error. FS is defined as the factor of safety. This was added to the equation to ensure that a suitably long runway was selected, even in the event of a mishap or miscalculation. An assumed value for the takeoff distance is indicated in the Specifications section of this report.

The wingspan was selected at 1 meter for two reasons: logistics and bending moment. The former was a limitation in order to indicate that the aircraft would be capable of fitting into a normal vehicle for transportation to test sites. The latter was to limit the bending moment acting on the wings. The tail length was determined by applying theoretical calculations from Aircraft Design: A Systems Engineering Approach (Sadraey, 2013). These equations, however, assume that the fuselage continues the entire length of the aircraft. For this case, though, that is not the case. Rather, the fuselage is approximately half of the length, with the other half being carbon fiber rods. The calculations indicated that the tail length be between 0.7 meters and 2.1 meters. The design team decided instead to design the tail to be 0.5 meters in order to keep the center of gravity forward. The tail section wings were designed to be two thirds of the aspect ratio of the main wing, which is a general rule for aviation (Sadraey, 2019, p.312). Finally, the tail height was chosen to be the smallest possible that would still clear the top of the main wing. By designing it in this way, a portion of the tail is able to flow through laminar air that has not been disturbed by the main wing.

Because most of the aircraft is 3D printed, there are only two other components in the structural design. The first is M5 screws which are 8 millimeters in length, have a thread diameter of 5 millimeters, and a 4 millimeter Allen Hex Drive. The second standard component is the carbon fiber rod used to reinforce the aircraft. These rods are 0.188 inches and 0.210 inches in diameter. Depending on the application, each rod varies in length.

The aircraft is assembled by means of constructing the bottom half of the fuselage and wings. Parts mate together in male-female interfaces and some parts are mated with screws. Once this is completed, the aircraft is wired with all its electrical components. This is done to allow ample room for the assemblers to insert and connect wires. After all electronics have been properly installed, the rest of the drone is assembled and fastened together. Once the aircraft will not require any further modifications, the plastic wrap is applied. This is done carefully in order to create air holes near the front and rear of the fuselage. The air holes cool the engine and ESC, which dissipate large amounts of heat during normal operation. Any cosmetic features such as flags and logos should be applied prior to the wrapping of the aircraft in plastic. Figure 17 shows the completely assembled aircraft without the ARSS parachute.

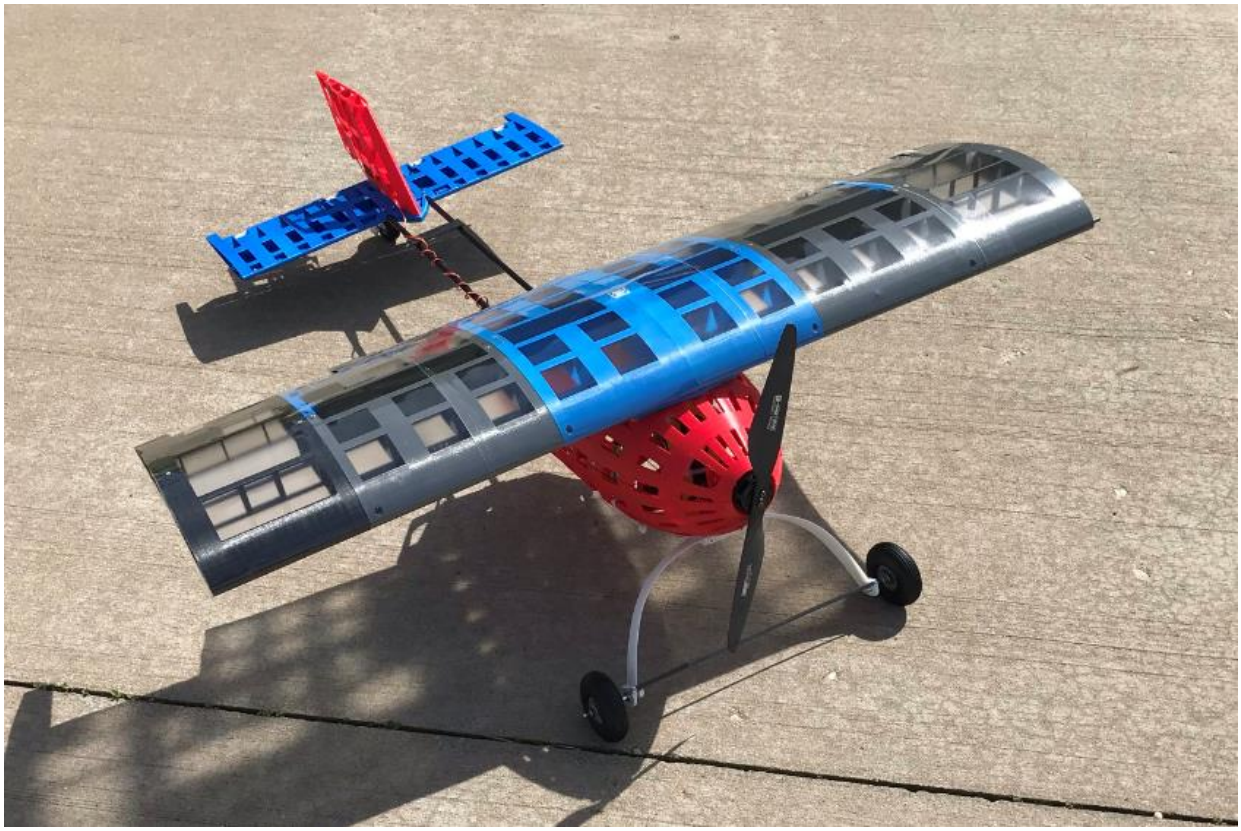

*Figure 17*. Assembled drone without ARSS parachute.

The electrical architecture of the aircraft features many components. A wiring diagram of the aircraft without the ARSS can be seen in Figure 18. Electrical current is supplied from the 5800 mAh battery and directed to the ESC. There, the current and voltage are transformed based on the electrical needs of the remaining components. The electric motor receives a 22.2 volt feed that can reach as high as 13.7 amperes for maximum throttle. The ESC also steps down power sent to the receiver, which sends signals to the main motor and control surface servomotors. All input control comes from the transmitter used by the pilot.

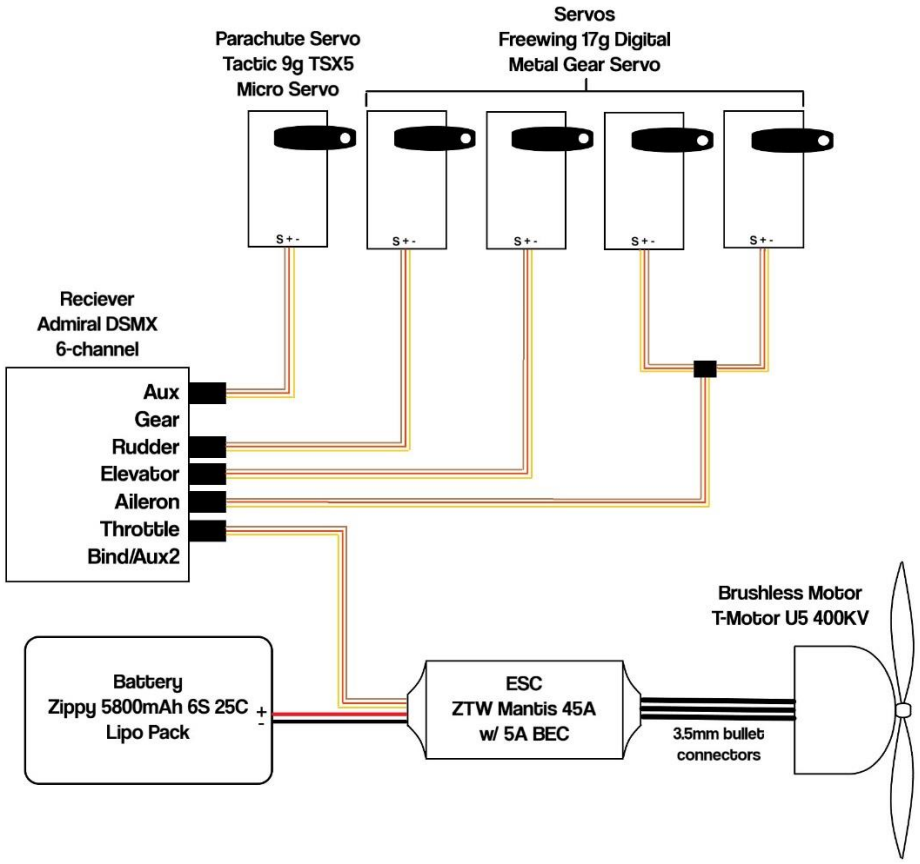


*Figure 18*. Wiring diagram of the aircraft omitting the ARSS.

Figure 19 is the wiring diagram for the complete aircraft including the ARSS. This wiring diagram is made separate in the event that the ARSS is not desired for a given unit.

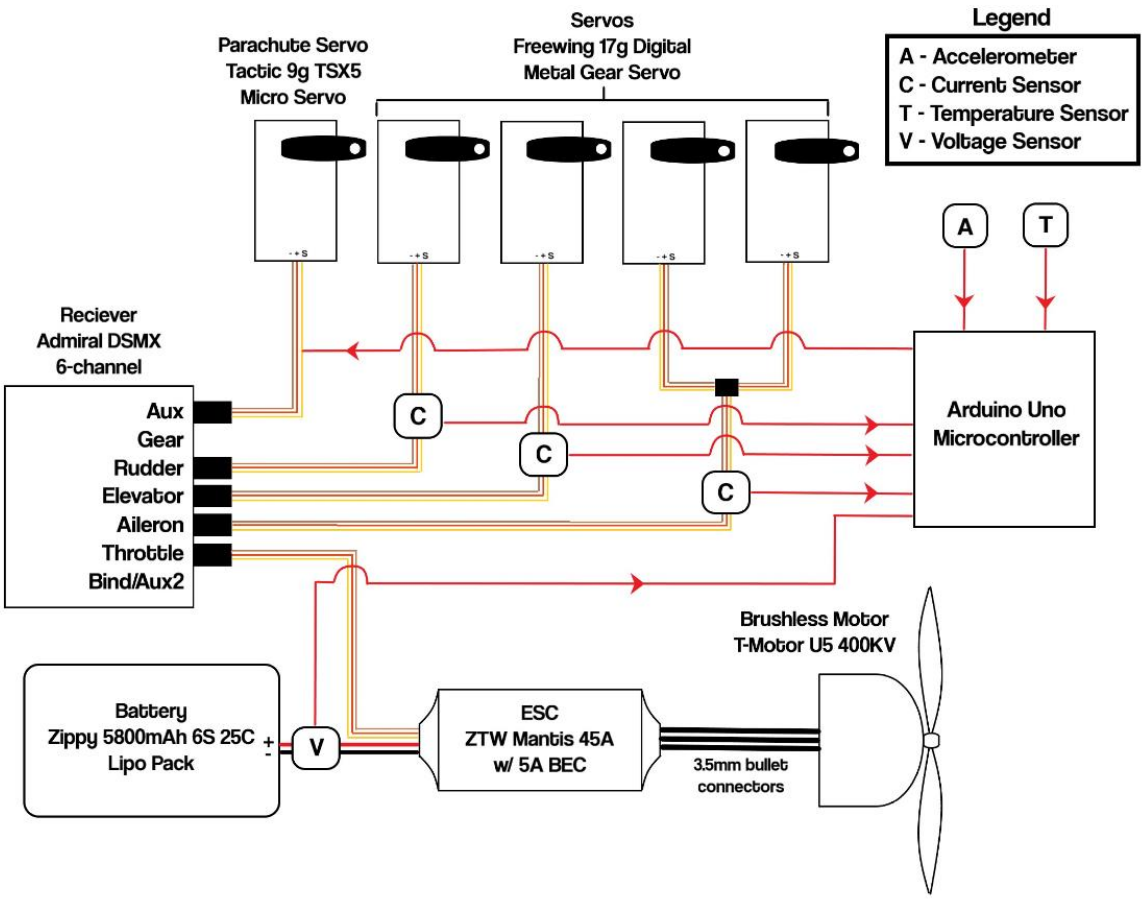


*Figure 19*. Wiring diagram for complete aircraft including the ARSS.

The three control surfaces implemented into the design of the aircraft are the rudder, elevator, and ailerons. Each surface has its own dedicated DC servomotor that controls the surface's angular position. By manipulating the position of the rudder, elevator, and ailerons, the aircraft's yaw, pitch, and roll can be controlled, respectively. Moving a given surface away from its equilibrium position generates a drag force that induces a corresponding moment. This phenomenon reorients the aircraft in a manner that is desired by the pilot. Because strong control inputs at high speeds can cause large normal accelerations, the ARSS is used to prevent the pilot from mistakenly overmaneuvering the aircraft.

The bill of material for the aircraft can be seen in Appendix I. It accounts for all materials, structural and electronic. The Unit Cost column indicates the cost per aircraft manufactured while the Total Cost column indicates the cost incurred by the design team. Certain expenses, such as the battery charger and transmitter were one-time expenditures because one is not needed for each successive unit built. Furthermore, there are components such as sensors that came in bulk packages; however, not all the sensors in the package are needed for one unit.

Appendix I contains the same list but with links to where each item can be purchased and technical specifications thereof. Various engineering drawings, exploded drawings, views from CAD, and photographs of the physical aircraft can be seen in Appendix J.

The cost of the aircraft quickly became larger than anticipated, at $498.55. This is because of the many constraints of the project. The requirement to 3D print incurred substantial material costs in addition to heavy weights. The payload also contributed to this large weight. As a result, the aircraft had to be powered by a $120 motor in order to achieve acceptable performance. Although the final design came in over budget, the design team nevertheless implemented the ARSS. At just $28.37, the dramatic increase in safety immediately justified the frivolous increase in cost.

As previously discussed, all calculations were carried out in MATLAB. This is due to the highly variable nature of aircraft. Changing the value of one parameter can change the values of many others. For this reason, a computer was used to execute all calculations. Values of some of these calculations can be seen in the Performance Capabilities section of this report. All the equations used can be seen in either Appendices D or E.

Autonomous Robotic Safety System

To correctly identify dangerous flight conditions, various sensors were installed in the ARSS. Table 3 provides the possible failure modes and detection methods.

Table 3

*ARSS Failure Mode Mitigations and Detection Methods*

| Failure Mode | Sensor Used | Detection |
|---|---|---|
| Low battery | Voltage sensor | Low voltage (18 V) coming from battery |
| Out of range | Current sensors | No additional current supplied to control surface servomotors for 20 seconds |
| Electrical disconnection | Current sensors | No current supplied to control surface servomotors at all |
| Over-maneuvered | Accelerometer | Accelerations greater than or equal to 3 g's |
| Overheated | Temperature sensor | Temperatures in the fuselage in excess of 120 degrees F |

As discussed previously, the ARSS cost only $28.37 to implement into each unit. With such a low cost and dramatic increase in safety, the design team decided to include it in the prototype unit. Sensors used can be found in Appendix I.

Calculations were performed in MATLAB to assist in the design of the ARSS parachute. To keep the aircraft descending straight down and not floating to the side, a relief hole was placed in the center of the parachute. The size of this hole was made to be 0.1 meters in diameter. Figure 20 provides the velocity response of parachutes of varying sizes.

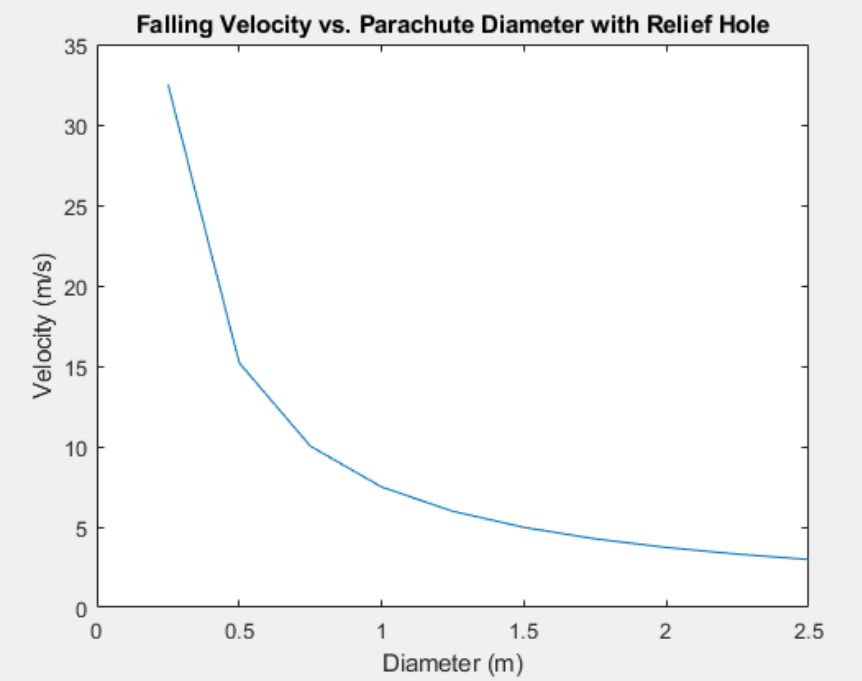


*Figure 19.* Falling velocity of the aircraft vs. Parachute diameter with a 0.1 m relief hole

By analyzing the graph, it was determined that there were minimal advantages to creating a parachute with a diameter in excess of 1.5 meters. This design would allow the aircraft to fall at approximately 5.0897 meters/second, or roughly 11.4 miles per hour. It was decided that this falling speed was satisfactory to not cause damage to the aircraft. The use of the parachute also allows the pilot to land the aircraft onto a specific surface that may be more conducive to such a landing.

**Specifications**

Table 4 indicates the specifications of the aircraft.

Table 4

*Specifications of the Aircraft*

| Parameter | Value | Units |
|---|---|---|
| Length | 1.143 | m |
| Wingspan | 1 | m |
| Empty mass | 4.214 | kg |
| Maximum payload weight | 2.2676 | kg |
| Maximum takeoff weight | 6.4816 | kg |
| Wing area | 1.143 | $m^2$ |
| Maximum thrust | 19.9143 | N |
| Wing coefficient of lift | 1.2 – 2.0 | --- |
| Coefficient of drag | 0.0297 | --- |
| Aspect ratio | 3.1250 | --- |
| Rudder range | [-25,25] | deg |
| Elevator range | [-25,20] | deg |
| Aileron range | [-30,30] | deg |

**Testing**

Because of the requirement to present the drone at the Mechanical Engineering Senior Design Showcase, it was decided by the team not to fly the aircraft prior to April 26, 2019. This decision allowed the team to guarantee that the aircraft would not be damaged for the event. Despite this, taxi tests were conducted. The aircraft was operated forward down a runway until the tail of the aircraft lifted off the pavement. This occurs once the aircraft is near takeoff speed. The aircraft was then promptly stopped.

These taxi tests not only validated the design's ruggedness, but that the aircraft had sufficient power to propel itself in its mission.

**Performance**

*Capabilities*

A list of performance capabilities can be found in Table 5. These values were theoretically obtained from the MATLAB program discussed in Appendix D.

Table 5

*Performance Capabilities of the Aircraft*

| Parameter | Value | Units |
|---|---|---|
| Stall speed | 32.2 | mph |
| Maximum speed | 283.3 | mph |
| Maximum Mach number | 0.37 | --- |
| Maximum range | 251.3 | mi |
| Maximum flight time | 84.8 | min |
| Minimum takeoff distance | 53.22 | ft |
| Maximum sustainable climb angle | 21.0 | degrees |

*Operation*

During takeoff, the aircraft should be pointed directly into the wind to maximize lift and minimize the risk of blowing off course. The throttle should be applied at 100 percent and the aircraft should proceed expediently toward the end of the runway with no turns made. Once the speed is great enough, the tail of the aircraft will lift off the ground. As the stall speed is reached and surpassed, the aircraft will pitch its nose up. This shall be aided by the pilot with the appropriate elevator application such that the aircraft climbs quickly over any potential objects such as structures or trees. In the event of an emergency, the ARSS parachute should be deployed immediately. The aircraft is not designed to have sufficient maneuverability to engage in demanding maneuvers and, therefore, should land via parachute rather than attempt to evade catastrophe.

Normal flight operations shall be conducted at such a height that there is no risk of colliding with ground objects such as trees and structures, yet low enough that the aircraft does not go out of range of the transmitter. In the event that the aircraft goes out of range, the ARSS will initiate an emergency landing. If the pilot performs too strenuous of a maneuver for the aircraft, the ARSS will also initiate an emergency landing in order to prevent the wings from tearing off.

There are two options for landing: parachute and conventional. The parachute should be used for landing whenever possible. This protocol helps the aircraft land more precisely and safely. A conventional landing must be executed at a higher-than-desired velocity due to the aircraft's lack of flaps. A high-speed conventional landing requires a long runway due to the lack of a braking feature. Despite this, it should be performed on a smooth surface in order to eliminate the possibility of bouncing during landing.

## Discussion

After all the specifications of the aircraft were determined, the MATLAB analyses were conducted to provide the performance metrics displayed in Table 5. These were then compared to the requirements of the project. The first requirement was that the aircraft be capable of carrying a payload of no less than 1.5 pounds. The theoretical calculations executed in MATLAB indicated that the drone could takeoff in 95 feet and at a maximum angle of 17 degrees with a 5 pound payload. While the performance would not be desirable, this payload can be achieved, dramatically surpassing the payload requirement for the project.

Furthermore, it was required that the drone be able to fly for no less than 20 minutes. This design, to the contrary, can remain airborne for nearly 85 minutes and cover a distance greater than 250 miles in this time. Therefore, the range is far in excess of the requirements. The aircraft was also primarily printed on a small 3D printer of approximately $300, which satisfies the manufacturing criteria of the project.

Moreover, the aircraft has a large amount of space for GPS equipment and or other computer equipment, making it capable of precision GPS guidance and Artificial Intelligence research. It is also easily replicable because of its simple design and fabrication style.

## Conclusion

For this project, the design team created a drone capable of delivering emergency supplies to individuals in distress. By using mathematics and principles of engineering, reasonable assurances were made that the aircraft produced at the end of the project would be suitable for its mission. There was no budget explicitly indicated, but it was desired to keep the cost near $300 to $400. The final budget of $498.55 exceeded that budget; however, the finished product delivered by the team greatly exceeded the requirements of the project. Because of this, the project can be deemed ultimately successful, and capable of one of the oldest and most sacred intentions of engineering – helping people.

## References

E423 Airfoil. (2019). In *Airfoil Tools*. Retrieved from http://airfoiltools.com/airfoil/details?airfoil=e423-il

Sadraey, M. H. (2013). *Aircraft Design: A Systems Engineering Approach* (pp. 265-340). Chichester, United Kingdom: Wiley & Sons, Ltd.

## Appendix

## Appendix A: Weighted Decision Matrix

| | | Parameter | 1st Level | 2nd Level | Contribution | Concept 1 Rating | Concept 2 Rating | Concept 1 Score | Concept 2 Score |
|---|---|---|---|---|---|---|---|---|---|
| Drone | Performance | Range | 40% | 60% | 24.00% | 6 | 8 | 1.44 | 1.92 |
| | | Speed | | 30% | 12.00% | 8 | 7 | 0.96 | 0.84 |
| | | Maneuverability | | 10% | 4.00% | 9 | 4 | 0.36 | 0.16 |
| | Safety | Target | 40% | 50% | 20.0% | 10 | 2 | 2 | 0.4 |
| | | Crash | | 50% | 20.0% | 10 | 2 | 2 | 0.4 |
| | Cost | Variable Cost | 20% | 70% | 14.00% | 8 | 4 | 1.12 | 0.56 |
| | | Fixed Cost | | 30% | 6.00% | 3 | 6 | 0.18 | 0.36 |

| | |
|---|---|
| Concept 1 | 8.06 |
| Concept 2 | 4.64 |

## Appendix B: DFMEA

| Expendable Drone Design Failure Mode and Effects Analysis | | | | | | | | | | | | Date | 3/26/2019 | |
|---|---|---|---|---|---|---|---|---|---|---|---|---|---|---|
| Part | Function | Requirements | Potential Failure Mode | Potential Effects of Failure Mode | Severity (1-5) | Potential Causes of Failure | Controls Prevention | Likelihood of Failure | Controls Detection | Design Prevention | Operation Prevention | ARSS Mitigation | Danger Factor | ARSS Danger Factor |
| Engine | Provide torque for propeller | Have power, cool temperatures, secured | Loss of power | Plane enters glider mode | 4 | Battery failure, wiring failure, loss of signal | Voltage sensor | 2 Yes | N/A | | Limit flight times | 5 | 60% | 10% |
| | | | Fire on board or overheating | Plane enters glider mode and aircraft components may fail | 5 | Drawing excessive current, aircooling is clogged | Temperature sensor | 1 Yes | Air cooling | Limit throttle usage | | 4 | 60% | 20% |
| | | | Engine falls from mounting | Plane enters glider mode | 4 | Structural failure from excessive heat | N/A | 1 Yes | Mounting reinforced | Limit rapid throttling | | 1 | 50% | 40% |
| Wings | Provide lift | Secured, unbent | Wings break from mounting in shear | Complete loss of lift | 5 | Overmaneuvering, assembly error, manufacturing error | Accelerometer | 1 Yes | 4 M5 screws at mounting | Limit overmaneuvering | | 5 | 60% | 10% |
| | | | Wings fail in bending | Dramatic loss of lift and complete loss of control | 5 | Overmaneuvering, assembly error, manufacturing error | Accelerometer | 3 Yes | Wings reinforced with struts and a carbon fiber rod | Limit overmaneuvering | | 5 | 80% | 30% |
| Elevator | Provide pitch moment | Secured, connected (electronically) | Servo or linkage becomes unattached | Loss of elevator control | 4 | Structural/mating failure | Current sensors | 1 Yes | Designed ruggedly | N/A | | 2 | 50% | 30% |
| | | | Elevator has a loss of power | Loss of elevator control | 4 | Wiring failure, power failure, loss of signal | Current sensors | 3 Yes | Wiring secured | Keep in range, limit flight times | | 5 | 70% | 20% |
| Rudder | Provide yaw moment | Secured, connected (electronically) | Servo or linkage becomes unattached | Loss of rudder control | 3 | Structural/mating failure | Current sensors | 1 Yes | Designed ruggedly | N/A | | 2 | 40% | 20% |
| | | | Elevator has a loss of power | Loss of rudder control | 3 | Wiring failure, power failure, loss of signal | Current sensors | 3 Yes | Wiring secured | Keep in range, limit flight times | | 5 | 60% | 10% |
| Ailerons | Provide roll | Secured, connected (electronically) | Servo or linkage becomes unattached | Loss of aileron control | 2 | Structural/mating failure | Current sensors | 1 Yes | Designed ruggedly | N/A | | 2 | 30% | 10% |
| | | | Aileron has a loss of power | Loss of aileron control | 2 | Wiring failure, power failure, loss of signal | Current sensors | 2 Yes | Wiring secured | Keep in range, limit flight times | | 5 | 40% | -10% |
| Landing gear | Takeoff support | Secured | Landing gear breaks | Crash during takeoff, in flight stability reduced | 4 | Impact with items, poor connections | N/A | 1 No | Ruggedly designed | Avoid runway debris | | 1 | 50% | 40% |
| ARSS - Nano flight conditions | Analyze internal conditions | Powered, sensor failure | Nano loses power | ARSS inoperable | 2 | Wiring failure, power failure | N/A | 1 No | Ruggedly designed | N/A | | 0 | 30% | 30% |
| | | | Sensors do not report failures | ARSS is not completely effective - Danger Factors can revert to original non-ARSS values | 2 | Programming failure, poor connections, poor supplier quality | N/A | 1 No | Ruggedly designed | N/A | | 0 | 30% | 30% |
| Tail section | Provides control moments | Stay attached | Breaks off | Complete loss of control | 5 | Over maneuvering, poor assembly | Current sensors | 2 Yes | Carbon fiber used as stronger material, ruggedly designed | Limit overmaneuvering | | 4 | 70% | 30% |
| Fuselage | Provides housing for internal components | Must remain intact | Structural failure | Complete loss of control | 5 | Overmaneuvering, assembly error, manufacturing error | Many | 1 Yes | Ruggedly designed | Limit overmaneuvering | | 5 | 60% | 10% |
| Parachute | Provide drag in landing | Deploys properly, remains intact | Snags on door, tail, servo linkage | Parachute does not slow the descent | 4 | Quality of design, insufficient airspeed at time of deployment | N/A | 1 No | Door located in position to deter interferences | Deploy at proper speed | | 1 | 50% | 40% |
| | | | Parachtue breaks | Parachute does not slow the descent | 4 | Mounting or cord failures | N/A | 1 No | Ruggedly designed | N/A | | 1 | 50% | 40% |
| Receiver | Receive input signal and produce control signals | Powered, within range | Loss of power | Complete loss of control | 5 | Battery failure, wiring failure | Current sensors | 1 Yes | Ruggedly designed | N/A | | 5 | 60% | 10% |
| | | | Out of range | Complete loss of control | 5 | Aircraft maneuvered out of range | Current sensors | 2 Yes | N/A | Limit range | | 5 | 70% | 20% |

| | | | | | | | | | | | | | | |
|---|---|---|---|---|---|---|---|---|---|---|---|---|---|---|
| Battery | Provide eletrical power to entire aircraft | Remains sufficiently charged, cooled | Low battery | Partial loss of control | 4 | Battery dies from excessive use | Voltage sensor | 2 | Yes | N/A | Be aware flight duration and aircraft response | 5 | 60% | 10% |
| | | | Overheated | Complete loss of control and fire/explosion | 5 | Battery is not sufficiently ventilated, overthrottling | Temperature sensor | 1 | Yes | Air cooling | Limit overmaneuvering | 5 | 60% | 10% |
| ESC | Regulate current drawn by motor | Remains wired, cooled | Loss of power/communication | Complete loss of control | 5 | Wiring failure | Current sensors | 1 | Yes | Ruggedly designed | N/A | 5 | 60% | 10% |
| | | | Overheated | Complete loss of control | 5 | Poor cooling | Many | 3 | Yes | Air cooling | N/A | 5 | 80% | 30% |
| Transmitter | Send control signals to aircraft | Powered, in range | Transmitter loses power | Complete loss of control | 5 | Transmitter malfunction or insufficient battery charge | Current sensors | 1 | Yes | N/A | Change batteries frequently | 4 | 60% | 20% |
| | | | Transmitter out of range | Complete loss of control | 5 | Flying aircraft out of range | Current sensors | 2 | Yes | N/A | Limit range | 5 | 70% | 20% |
| | | | | | | | | | | | | | 0% | 0% |

# Appendix C: PLA Material Specifications

| Mechanical Properties | Metric | English | Comments |
|---|---|---|---|
| Hardness, Shore A | 67.0 - 85.0 | 67.0 - 85.0 | Average value: 76.3 Grade Count:3 |
| Hardness, Shore D | 59.0 - 77.0 | 59.0 - 77.0 | Average value: 65.8 Grade Count:5 |
| Tensile Strength, Ultimate | 14.0 - 114 MPa | 2030 - 16500 psi | Average value: 46.8 MPa Grade Count:92 |
| Film Tensile Strength at Yield, MD | 19.0 - 54.0 MPa | 2760 - 7830 psi | Average value: 30.5 MPa Grade Count:13 |
| Film Tensile Strength at Yield, TD | 14.0 - 48.0 MPa | 2030 - 6960 psi | Average value: 26.5 MPa Grade Count:13 |
| Tensile Strength, Yield | 2.00 - 103 MPa | 290 - 14900 psi | Average value: 37.5 MPa Grade Count:28 |
| Film Elongation at Break, MD | 160 - 600 % | 160 - 600 % | Average value: 326 % Grade Count:16 |
| Film Elongation at Break, TD | 100 - 640 % | 100 - 640 % | Average value: 402 % Grade Count:16 |
| Elongation at Break | 0.500 - 700 % | 0.500 - 700 % | Average value: 62.9 % Grade Count:114 |
| Elongation at Yield | 2.00 - 400 % | 2.00 - 400 % | Average value: 60.2 % Grade Count:20 |
| Modulus of Elasticity | 0.0850 - 13.8 GPa | 12.3 - 2000 ksi | Average value: 2.80 GPa Grade Count:86 |
| Tenacity | 0.177 - 0.441 N/tex | 2.00 - 5.00 g/denier | Average value: 0.296 N/tex Grade Count:9 |
| Flexural Yield Strength | 6.00 - 145 MPa | 870 - 21000 psi | Average value: 77.4 MPa Grade Count:71 |
| Flexural Modulus | 0.215 - 13.8 GPa | 312 - 2000 ksi | Average value: 3.86 GPa Grade Count:72 |
| Secant Modulus, MD | 3.30 - 3.44 GPa | 479 - 499 ksi | Average value: 3.36 GPa Grade Count:3 |
| Secant Modulus, TD | 3.78 - 3.90 GPa | 549 - 566 ksi | Average value: 3.85 GPa Grade Count:3 |
| Izod Impact, Notched | 0.128 - 8.54 J/cm | 0.240 - 16.0 ft-lb/in | Average value: 1.39 J/cm Grade Count:47 |
| Izod Impact, Unnotched | 2.67 - 5340 J/cm | 5.00 - 10000 ft-lb/in | Average value: 6.19 J/cm Grade Count:35 |
| Charpy Impact, Unnotched | 0.500 J/cm² - NB | 2.38 ft-lb/in² - NB | Average value: 2.39 J/cm² Grade Count:33 |
| Charpy Impact, Notched | 0.100 - 1000 J/cm² | 0.476 - 4760 ft-lb/in² | Average value: 0.768 J/cm² Grade Count:42 |
| Tear Strength | 65.0 - 90.0 kN/m | 371 - 514 pli | Average value: 76.7 kN/m Grade Count:3 |
| Elmendorf Tear Strength, MD | 0.0441 - 0.862 g/micron | 1.12 - 21.9 g/mil | Average value: 0.426 g/micron Grade Count:16 |
| Elmendorf Tear Strength, TD | 0.0361 - 1.28 g/micron | 0.918 - 32.6 g/mil | Average value: 0.510 g/micron Grade Count:16 |
| Dart Drop Total Energy | 240 - 420 J/cm | 0.450 - 0.787 ft-lb/mil | Average value: 347 J/cm Grade Count:3 |
| Film Tensile Strength at Break, MD | 19.0 - 110 MPa | 2760 - 16000 psi | Average value: 43.7 MPa Grade Count:13 |
| Film Tensile Strength at Break, TD | 13.0 - 145 MPa | 1890 - 21000 psi | Average value: 50.5 MPa Grade Count:13 |

| Thermal Properties | Metric | English | Comments |
|---|---|---|---|
| Melting Point | 90.0 - 180 °C | 194 - 356 °F | Average value: 157 °C Grade Count:78 |
| Maximum Service Temperature, Air | 60.0 - 240 °C | 140 - 464 °F | Average value: 180 °C Grade Count:16 |
| Deflection Temperature at 0.46 MPa (66 psi) | 50.0 - 160 °C | 122 - 320 °F | Average value: 80.3 °C Grade Count:69 |
| Deflection Temperature at 1.8 MPa (264 psi) | 50.0 - 149 °C | 122 - 300 °F | Average value: 82.6 °C Grade Count:19 |
| Vicat Softening Point | 44.0 - 130 °C | 111 - 266 °F | Average value: 71.7 °C Grade Count:28 |
| Glass Transition Temp, Tg | -43.0 - 120 °C | -45.4 - 248 °F | Average value: 52.6 °C Grade Count:42 |
| Flammability, UL94 | HB - V-0 | HB - V-0 | Grade Count:11 |

## Appendix D: MATLAB Program

```
%   Drone Senior Design MATLAB Analysis Tool
%   This tool is to be used to perform dynamic and static analysis of a
%   senior design project 3D printed drone.
%   The program is designed to act as a GUI formatted with IF statements.
%   Matthew Chapman, Cameron Barr, and Nathan Knutty
%   Advisors: Dr. Rob Williams, Dr. Shao Wang
%   Readers: Dr. Daniel Deckler and Dr. S. Graham Kelly
%   12/18/2018 AD

%   Setup
close all
clear all
clc
disp('Welcome to the Senior Design Analysis Tool')
disp('This program provides analysis of various flight characteristics of the
aircraft')

%   Provide input values
ma = 4.214;     %kg mass of aircraft
mp = 1.5/2.205;     %kg mass of payload lbf-kg conv
m = ma + mp;    %mg complete mass of loaded system
rho = 1.204;    %kg/m^3 density of air at STP
g = 9.81;   %m/s^2 accel due to gravity
nu = 14.88*10^-6;   %m^2/s dynamic viscosity
FS = 1.2;   %factor of safety
a = 343;    %m/s speed of sound at sea level and STP
%wings
b = 1;  %m wingspan
c = 8/39.37;     %m wing chord
Cl = 1.2;   %coefficient of lift for NACA E423
Cl_to = 2;   %coefficeient of lift for takeoff of NACA E423
wt = 0.037;    %m wing thickness projected
AR = b/c;   %aspect ratio for wing
%tail
b_tail = 6/39.37;   %m tail wingspan
c_tail = 3/39.37;   %m tail wing chord
Cl_tail = 1.2;  %coefficient of lift of tail airfoil NACA 2412
wt_tail = 1/39.37;  %m thickness of tail wing
Kc = 1.4;   %correction factor for optimal tail arm length
D_aft_fus = 2*0.5/39.37;  %m diameter of fuselage at aft location
%aircraft
Dmajfus = 8/39.37;   %m (in/conv) fuselage major diameter
Dminfus = 8/39.37;  %m (in/conv) fuselage minor diameter
Cd = 0.027*1.10;  %coefficient of drag (Cessna 172 + 10% for conservative
guess)
mu_fric = 0.02;  %coefficient of friction of aircraft on ground (grass)
%engine
maxrpm = 6950;  %rpm max rpm of motor
Dprop = 14/39.37;     %m (in/conv) diameter of propeller
ppitch = 4.8/39.37;    %m (in/conv) pitch of propeller

%   Drivetrain information
%   T-Motor U5 KV400
```

```
%   14" T-Motor prop w/ pitch 4.8"
throttle = [50 65 75 85 100]; %percent
current_eng = [3.4 6.3 8.5 11.4 13.7];  %Amps
power_eng = [75.8 139.86 188.70 253.08 304.14]; %Watts
thrust_eng = g*[0.8 1.2 1.5 1.82 2.03];   %N thrust was given in kg so it is
multiplied by g to get Force
rpm_eng = [4300 5400 5900 6500 6950];   %rpm

%   Area calculations
Aw = b*c;   %m^2 wingspan*chord surface area for lift
Aa = (pi/4)*Dmajfus*Dminfus;    %m projected area of fuselage

%   Parachute information
Cdpara = 1.75;  %coefficient of drag of parachute (assumed from NASA)
Dpara_vector = 0.25:0.25:2.5;   %m diameter of parachute
Dpara_hole = 0.1;   %m diameter of hole in parachute

%   Setup menu for GUI
flag = menu('What analysis would you like to perform?','Stall Speed
Calculation','Steady State Velocity Calculator','Free Body Analysis','Wing
Turbulence Analysis','Battery Life and Range Analysis','Takeoff Distance
Analysis','Climb Analysis','Wing Loading Analysis','Tail Design
Analysis','Parachute Design')
%'flag' indicates the menu option selected

%   Stall speed analysis
if flag == 1;
    disp('Stall Speed Analysis')
    %   Calculate values
    Ts = (Aa*Cd*m*g)/(Aw*Cl);
    Vs = sqrt((2*m*g)/(rho*Aw*Cl));
    %   Present values
    parameter = 'Ts, Vs';
    Parameter = string(parameter);
    value = [Ts Vs];
    Value = string(value);
    units = 'N, m/s';
    Units = string(units);
    tab11 = table(Parameter,Value,Units)
    %   Present stall speed in mph
    ss_mph = Vs*2.237;
    formatspec = 'The stall speed is %4.1f mph';
    fprintf(formatspec,ss_mph)

%   Steady State Velocity Calculator
elseif flag == 2;
    disp('Steady State Velocity Calculator')
    %determine eop
    eop = menu('Specify Engine Output
Percentage','50%','65%','75%','85%','100%');
    %index thrust
    thrust = thrust_eng(eop);
    %calculate steady state speed
    v_ss = sqrt((2*thrust)/(rho*Aa*Cd))   %m/s steady state speed
    %convert sss to mph
    sss_mph = v_ss*2.237;
```

```
    Ma = v_ss/a;    %Mach number
    formatspec = 'The steady state velocity is %4.1f mph and Mach %3.2f';
    fprintf(formatspec,sss_mph,Ma)

    %   Free Body Analysis
elseif flag == 3;
    disp('Free Body Analysis')
    %determine eop
    eop = menu('Specify Engine Output
Percentage','50%','65%','75%','85%','100%');
    %index thrust
    thrust = thrust_eng(eop);
    %calculate steady state speed
    v_ss = sqrt((2*thrust)/(rho*Aa*Cd))   %m/s steady state speed
    %four forces calculation
    W = m*g;    %N force of weight
    L = (1/2)*rho*Aw*Cl*(v_ss^2);   %N lift force
    T = thrust;    %N thrust from propeller
    D = (1/2)*rho*Aa*Cd*(v_ss^2);   %N drag force
    %present resultant forces
    disp('Force values in units N (Newtons)')
    tab31 = table(W,L,T,D)
    %present resultant accelerations
    ay = ((L - W)/m)/g; %g's of acceleration in y-direction
    ax = ((T - D)/m)/g; %g's of acceleration in x-direction
    disp('Resultant accelerations in x,y-directions in units of g')
    tab32 = table(ay,ax)

    %   Wing Turbulence Analysis
elseif flag == 4;
    disp('Wing Turbulence Analysis')
    %determine eop
    eop = menu('Specify Engine Output
Percentage','50%','65%','75%','85%','100%');
    %index thrust
    thrust = thrust_eng(eop);
    %calculate steady state speed
    v_ss = sqrt((2*thrust)/(rho*Aa*Cd))   %m/s steady state speed
    %calculate Reynolds Number
    Re = v_ss*c/nu;
    Re_avg = Re/2;
    formatspec = 'The Reynolds number is %10.0f and the average Reynolds
number is %10.0f';
    fprintf(formatspec,Re,Re_avg)
    disp(' ')
    if Re >= 5*10^5;
        disp('Airflow over wings is TURBULENT')
    else
        disp('Airflow over wings is laminar')
    end

    %   Battery Life and Range Analysis
elseif flag == 5;
    disp('Battery Life and Range Analysis')
    %determine eop
```

```
    eop = menu('Specify Engine Output
Percentage','50%','65%','75%','85%','100%');
    %Determine average current drawn for operation
    I_eng = current_eng(eop);   %Amp
    num_servos = 4; %Ea number of servomotors used by aircraft
    servo_op_perc = 50; %perc utilization of servos during average flight
    I_servos = 0.120*(servo_op_perc/100)*num_servos + 0.020*(1 -
(servo_op_perc/100))*num_servos;  %Amp avg current drawn by servos -
current_per_servo*operation_perc*num_servos
    %Overall operation current drawn includes engine current and current
    %drawn by servomotors
    I_overall = I_eng + I_servos;  %Amp Overall operation current drawn
includes engine current and current drawn by servomotors
    batt_cap = 5.2; %AmpHr combined capacity of batteries for use by aircraft
    batt_dur = batt_cap/I_overall;  %Hr duration of battery (time)
    batt_dur_minu = batt_dur*60;    %min time (in minutes) for estimated
duration of battery
    %Steady state velocity calculation for this battery duration
    %index thrust
    thrust = thrust_eng(eop);
    %calculate steady state speed
    v_ss = sqrt((2*thrust)/(rho*Aa*Cd));   %m/s steady state speed
    %convert sss to mph
    sss_mph = v_ss*2.237;
    %calculate distance traveled
    batt_dist = sss_mph*batt_dur;   %mi distance traveled for battery
duration
    formatspec = 'The battery duration is estimated to be %4.1f minutes
operating at %4.1f mph over a distance of %5.1f miles';
    fprintf(formatspec,batt_dur_minu,sss_mph,batt_dist)

    %   Takeoff Distance Analysis
elseif flag == 6;
    disp('Takeoff Distance Analysis')
    eop = menu('Specify Engine Output
Percentage','50%','65%','75%','85%','100%');
    %index thrust
    thrust = thrust_eng(eop);   %kg thrust in KG!!!
    T = thrust; %N force of thrust
    to_dist_m = (FS*g*m^2)/((rho*Aw*Cl_to)*(T - ((Aa*Cd*m*g)/(Aw*Cl_to)) -
mu_fric*m*g));  %m takeoff distance in meters
    to_dist_ft = to_dist_m*3.281; %ft takeoff distance in feet
    formatspec = 'The minimum takeoff distance is %5.2f feet';
    fprintf(formatspec,to_dist_ft)

    %   Climb Analysis
elseif flag == 7;
    disp('Climb Analysis')
    disp('Angle of attack can be specified for analysis or a generic graph
can be formulated')
    eop = menu('Specify Engine Output
Percentage','50%','65%','75%','85%','100%');
    %index thrust
    thrust = thrust_eng(eop);   %kg thrust in KG!!!
    T = thrust; %N force of thrust
    %   Allow user to specify angle of attack or generate steady state
```

```
    %   speed graph with respect to theta
    choice71 = menu('Would you like to specify the Angle of Attack or
generate a graph for speeds?','Specify Angle of Attack','Generate graph')
    if choice71 == 1;
        disp('Angle of Attack Specified')
        choice72 = input('Specify Angle of Attack in degrees >: ');
        theta = choice72;   %Redefine choice72 as angle of attack theta
        %steady state speed calculation
        v_ss = sqrt((T - m*g*sind(theta))./(0.5*rho*Aa*Cd));    %m/s steady
state speed in m/s
        v_ss_mph = v_ss*2.237;  %mph steady state speed in mph
        %stall speed calculation
        v_s = sqrt((2*m*g*cosd(theta))/(rho*Aw*Cl));    %m/s stall speed in
m/s
        v_s_mph = v_s*2.237;    %mph stall speed in mpg
        formatspec = 'The steady state speed is %4.1f mph and the stall speed
is %4.1f mph';
        fprintf(formatspec,v_ss_mph,v_s_mph)
        %compare stall speed to steady state speed
        if v_ss >= v_s;
            disp('Flight conditions are stable')
            disp('Thrust is sufficient to sustain angle of attack without
stalling')
        elseif v_ss < v_s;
            disp('FLIGHT CONDITIONS ARE NOT STABLE!')
            disp('!!! CATESTROPHIC FAILURE IMMINENT !!!')
            error('Steady state speed is less than stall speed')
        end
    elseif choice71 == 2;
        disp('Graph of speeds generated')
        theta = -90:1:90; %deg define theta as the angle of attack ranging
from all possible values
        v_ss = sqrt((T - m*g*sind(theta))./(0.5*rho*Aa*Cd));    %m/s steady
state speed in m/s
        v_ss_mph = v_ss*2.237;  %mph steady state speed in mph
        %stall speed calculation
        v_s = sqrt((2*m*g*cosd(theta))/(rho*Aw*Cl));    %m/s stall speed in
m/s
        v_s_mph = v_s*2.237;    %mph stall speed in mph
        %plot results
        plot(theta,v_ss_mph,theta,v_s_mph,'--')
        title('Steady State Speed and Stall Speed vs Angle of Attack')
        xlabel('Angle of Attack (deg)')
        ylabel('Speed (mph)')
        ylim([-5 50])
        legend('Steady State Speed','Stall Speed')
    end

    %   Wing Loading Analysis
elseif flag == 8;
    disp('Wing Loading Analysis')
    disp('This provides a structural analysis of the drag forces acting on
the wings at a given speed.')
    disp('Because of the statically indeterminant design of the wings, an
analysis cannot be completed.')
    disp('Destructive testing will be completed to determine maximum bending
moment.')
```

```
    %   Tail Design Analysis
elseif flag == 9;
    disp('Tail Design Analysis')
    disp('Volume coefficient should be selected between 0.5 and 1.1')
    Vh = input('Specify volume coefficient >: ');   %Volume coefficient
should be selected between 0.5 and 1.1
    b_tail = (((2*b)/(3*c))*c*Aw*Vh)^(1/3); %m calculates the tail span using
ARt = 2/3 * ARw
    c_tail = (3*b_tail*c)/(2*b);    %m calculates the tail chord using ARt =
2/3 * ARw
    tail_m = [b_tail c_tail]';  %m matrix of tail dimensions for table
    formatspec = 'The span of the tail is %3.3f m and the chord of the tail
is %3.3f m';
    fprintf(formatspec,b_tail,c_tail)
    disp(' ')
    b_tail_in = b_tail*39.37;   %in
    c_tail_in = c_tail*39.37;   %in
    tail_in = [b_tail_in c_tail_in]';   %in matrix of tail dimensions for
table
    formatspec92 = 'The span of the tail is %3.1f in and the chord of the
tail is %3.1f in';
    fprintf(formatspec92,b_tail_in,c_tail_in)
    tail_dim = 'bc';
    Tail_dim = tail_dim';
    tab91 = table(Tail_dim,tail_m,tail_in),
    disp(' ')
    %tail arm length calculations
    disp('Tail Arm Length Calculations')
    l_ta = Kc*sqrt((4*c*Aw*Vh)/(pi*D_aft_fus)); %m optimal length of tail arm
    l_ta_in = l_ta*39.37;   %in optimal length of tail arm in inches
    formatspec93 = 'The optimal length of the tail arm is %4.3f m or %4.1f
in';
    fprintf(formatspec93,l_ta,l_ta_in)
    disp(' ')
    %vertical tail
    disp('Vertical Tail Analysis')
    disp('The maximum angle of attack should be specified approximately
around 10 degrees')
    alpha = input('Specify maximum angle of attack of horizontal tail >: ');
%deg angle of attack
    y_stall = c*sind(alpha);   %m determines stall height of fin due to
washout from horizontal members during a climb
    tail_h_ratio = 3;   %ratio of stall portion height to washed-out portion
height
    h_tail = y_stall*(tail_h_ratio + 1);     %m height of vertical stabilizer
forced at three times stall height
    base_tail = 1.5*c_tail; %m base of tail forced to be half of horizontal
stabilizer chord
    top_tail = (3/4)*base_tail;    %m top of tail forced to be 1/4 horiz
stabilizer chord and 1/2 of base chord
    A_tail = ((base_tail + top_tail)/2)*h_tail;  %m^2 total area of vertical
tail member
    theta = atand(((h_tail)*c_tail*sind(alpha))/(base_tail - top_tail));
%deg angle of tail vertical stabilizer
    theta_prime = 90 - theta;   %deg complimentary angle of theta used to
analyze stall portion
```

```
    A_tail_stall = ((base_tail - c_tail*sind(alpha)*tand(theta_prime) +
top_tail)/2)*(h_tail - y_stall);  %m^2 area of tail vertical stabilizer not
stalled
    stall_ratio = 100*A_tail_stall/A_tail  %perc ratio of stalled to
unstalled
    disp('The stall ratio should be approximately 50%')
    disp('To increase the stall ratio, either increase the tail h ratio or
increase the top tail ratio')
    formatspec94 = 'The height of the tail is %4.3f m';
    fprintf(formatspec94,h_tail)
    disp(' ')
    %base of tail
    formatspec95 = 'The base of the tail is %4.3f m';
    fprintf(formatspec95,base_tail)
    disp(' ')
    %top of tail
    formatspec96 = 'The top of the tail is %4.3f m';
    fprintf(formatspec96,top_tail)
    %display results tabularly
    dimension = 'hbt';
    Dimension = dimension'; %these vectors simply display variable names for
use in the table ^^
    tail_vert_dim = [h_tail base_tail top_tail]';    %m dimensions of
vertical portion of tail
    tail_vert_dim_in = 39.37*tail_vert_dim;
    disp('Tail dimensions in meters and inches')
    tab92 = table(Dimension,tail_vert_dim, tail_vert_dim_in)

elseif flag == 10;
    disp('Parachute Design')
    choice101 = menu('Select an option','Plot Values','Calculate Diameter');
    if choice101 == 1;
        v_para = sqrt((8*m*g)./(pi*rho*Cdpara*(Dpara_vector.^2 -
Dpara_hole^2)));
        figure
        plot(Dpara_vector,v_para)
        title('Falling Velocity vs. Parachute Diameter with Relief Hole')
        xlabel('Diameter (m)')
        ylabel('Velocity (m/s)')
        T101 = table(Dpara_vector',v_para')
    elseif choice101 == 2;
        v_para = input('Specify desired impact velocity (m/s) >: ');
        Dpara = sqrt(((8*m*g)/((v_para^2)*pi*rho*Cdpara)) + Dpara_hole^2);
        formatspec101 = 'The required parachute diameter is %2.1f m';
        fprintf(formatspec101,Dpara)
    end
end
```

## Appendix E: Equations

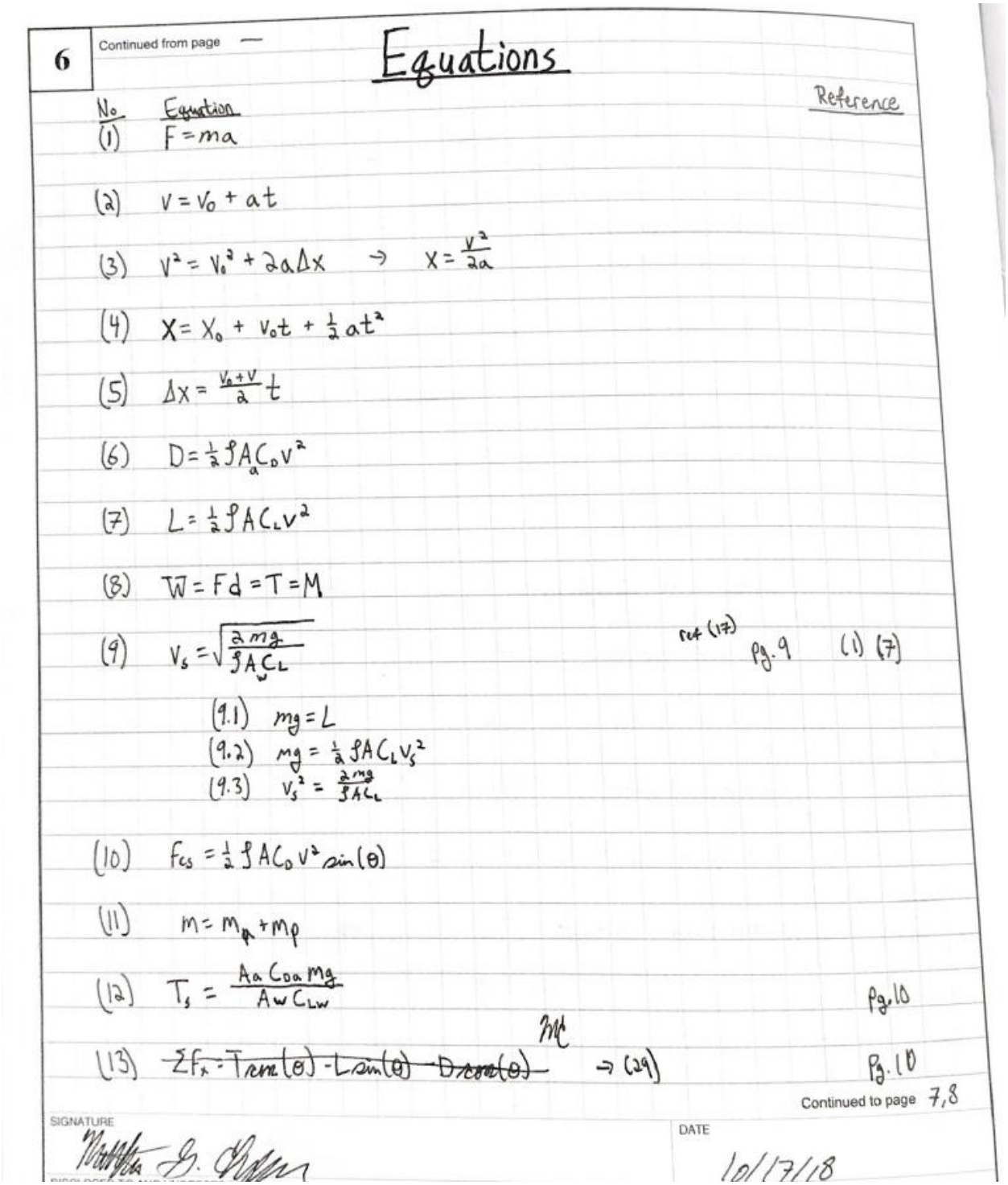

6 Continued from page —

# Equations

| No. | Equation | Reference |
|---|---|---|
| (1) | $F = ma$ | |
| (2) | $v = v_0 + at$ | |
| (3) | $v^2 = v_0^2 + 2a\Delta x \rightarrow x = \frac{v^2}{2a}$ | |
| (4) | $X = X_0 + v_0 t + \frac{1}{2}at^2$ | |
| (5) | $\Delta x = \frac{v_0 + v}{2} t$ | |
| (6) | $D = \frac{1}{2}\rho A_a C_D v^2$ | |
| (7) | $L = \frac{1}{2}\rho A C_L v^2$ | |
| (8) | $W = Fd = T = M$ | |
| (9) | $v_s = \sqrt{\frac{2mg}{\rho A_w C_L}}$ | ref (17) pg. 9 (1) (7) |
| (9.1) | $mg = L$ | |
| (9.2) | $mg = \frac{1}{2}\rho A C_L v_s^2$ | |
| (9.3) | $v_s^2 = \frac{2mg}{\rho A C_L}$ | |
| (10) | $f_{cs} = \frac{1}{2}\rho A C_D v^2 \sin(\theta)$ | |
| (11) | $m = m_A + m_p$ | |
| (12) | $T_s = \frac{A_a C_{Da} m g}{A_w C_{Lw}}$ | pg. 10 |
| (13) | ~~$\Sigma F_x = T\cos(\theta) - L\sin(\theta) - D\cos(\theta)$~~ $\Rightarrow$ (29) | pg. 10 |

Continued to page 7,8

SIGNATURE [signature] DATE 10/17/18

| No | Equation | Reference |
|---|---|---|
| ~~(14)~~ | $\sum F_x = T\cos(\theta) - \frac{1}{2}\rho v^2[A_w C_{Lw}\sin(\theta) - A_a C_{Da}\cos(\theta)]$ | pg. 10 |
| ~~(15)~~ | $\sum F_y = T\sin(\theta) + L\cos(\theta) - D\sin(\theta) - W$ | pg. 11 |
| ~~(16)~~ | $\sum F_y = T\sin(\theta) - mg + \frac{1}{2}\rho v^2[A_w C_{Lw}\cos(\theta) - A_a C_{Da}\sin(\theta)]$ | pg. 11 |
| ~~(17)~~ | $V_s = \sqrt{\frac{2[mg - T\sin(\theta)]}{\rho[A_w C_{Lw}\cos(\theta) - A_a C_{Da}\sin(\theta)]}}$ | ref (9) pg. 11 (9) |
| (18) | $T_s = \frac{\rho}{2\cos(\theta)}\left[A_w C_{Lw}\sin(\theta) - A_a C_{Da}\cos(\theta)\right]\left[\frac{2(mg - T\sin(\theta))}{\rho(A_w C_{Lw}\cos(\theta) - A_a C_{Da}\sin(\theta)}\right]$ | (4) pg. 10 |
| (19) | $T = \frac{1}{2}\rho A_{prop} V_{air}^2$ | |
| (20) | $V_{ss} = \sqrt{\frac{2T}{\rho A_a C_D}}$ | ref (27) pg. 13 |
| (21) | $AR = \frac{b}{c}$ | pg. 14 |
| (22) | $Re = \frac{\rho u l}{\mu} = \frac{ul}{\nu}$ | |
| (23) | $t = \frac{\text{battle capacity}}{\text{current}}$ | |
| (24) | $X_{TO} = \frac{(FS)\, m^2 g}{(\rho A_w C_L)(T - D - \mu_F mg)}$ | pg. 19 |
| (25) | $X_{TO} = \frac{(FS)\, m^2 g}{(\rho A_w C_L)(T - \frac{A_a C_{Da} mg}{A_w C_L} - \mu_F mg)}$ | pg. 20 |

Continued to page 8

| No | Equation | Reference |
|---|---|---|
| (26) | $X_{TOWD} = \frac{(FS)\, m^2 g}{(\rho A_w C_L)(T - \mu_f mg)}$ | Pg. 20 |
| (27) | $V_{ss} = \sqrt{\frac{2T\cos(\theta)}{\rho[A_w C_{Lw} + A_a C_{Da}\cos(\theta)]}}$ | ref (21) Pg. 10 |
| (28) | $V_{ss} = \sqrt{\frac{T - mg\sin(\theta)}{\frac{1}{2}\rho A_a C_D}}$ | ref (27) Pg. 10, 21 |
| (29) | $\Sigma F_x = T - D - mg\sin(\theta)$ | Pg. 21 |
| (30) | $\Sigma F_y = L - mg\cos(\theta)$ | Pg. 21 |
| (31) | $V_s = \sqrt{\frac{2mg\cos(\theta)}{\rho A_w C_L}}$ | Pg. 21 |
| (32) | $\Sigma M = I\alpha$ | Pg. 22 |
| (33) | $A_{CS} = \frac{2I\alpha}{\rho \cos d\, v^2 \sin(\theta)}$ | Pg. 22 |
| (34) | $\alpha = \frac{\omega}{t}$ | Pg. 22 |
| (35) | $V_H = \frac{l\, S_w}{cs}$ | Pg. 24 |
| (36) | $AR_t = \frac{2}{3} AR_w$ | Pg. 24 |

SIGNATURE

Continued to page 34

DISCLOSED TO AND UNDERSTOOD BY

DATE 3/29/19

DATE

Continued from page

# Equations con't

| No | Equation | Reference |
|---|---|---|
| (37) | $C_t = \frac{3}{2}\frac{b_t c}{b}$ | Pg. 24 |
| (38) | $b_t = \sqrt[3]{\frac{2bcA_w V_H}{3c}}$ | Pg. 24 |
| (39) | $\ell_{.ta} = K_c\sqrt{\frac{4cA_w V_H}{\pi D_{tail}}}$ | Pg. 25 |
| (40) | $A_{stall} = \frac{1}{2}[base_t - C_t \sin(\alpha)\tan(\theta') + top_t][h_t - y_{stall}]$ | Pg. 25 |
| (41) | $V_{para} = \sqrt{\frac{8mg}{\pi\rho C_{Dpara}(D_{para}^2 - D_{hole}^2)}}$ | Pg. 33 |
| (42) | $D_{para} = \sqrt{\frac{8mg}{v^2\pi\rho C_{Dpara}} + D_{hole}^2}$ | Pg. 33 |
| (43) | $R_c = L$ | Pg. 36 |
| (44) | $M_{max} = \frac{L\ell}{2}$ | Pg. 36 |

## Appendix F: T-Motor Specifications

| Test Report | | | |
|---|---|---|---|
| Test Item | U5 KV400 | Report NO. | U.00002 |
| **Specifications** | | | |
| Internal Resistance | 116mΩ | Configuration | 12N14P |
| Shaft Diameter | 5mm | Motor Dimensions | Φ42.5×37.5mm |
| AWG | 16# | Cable Length | 600mm |
| Weight Including Cables | 195g | Weight Excluding Cables | 156g |
| No.of Cells (Lipo) | 3-8S | Idle Current@10v | 0.3A |
| Max Continuous Power 180S | 850W | Max Continuous Current 180S | 30A |

**Load Testing Data**

| Ambient Temperature | / | Voltage | DC Power Supplier |
|---|---|---|---|

| Item No. | Voltage (V) | Prop | Throttle | Current (A) | Power (W) | Thrust (G) | RPM | Efficiency (G/W) | Operating Temperature (℃) |
|---|---|---|---|---|---|---|---|---|---|
| | | T-MOTOR 14*4.8CF | 50% | 3.4 | 75.48 | 800 | 4300 | 10.60 | 45 |
| | | | 65% | 6.3 | 139.86 | 1200 | 5400 | 8.58 | |
| | | | 75% | 8.5 | 188.70 | 1500 | 5900 | 7.95 | |
| | | | 85% | 11.4 | 253.08 | 1820 | 6500 | 7.19 | |
| | | | 100% | 13.7 | 304.14 | 2030 | 6950 | 6.67 | |

## Appendix G: Climb Analysis

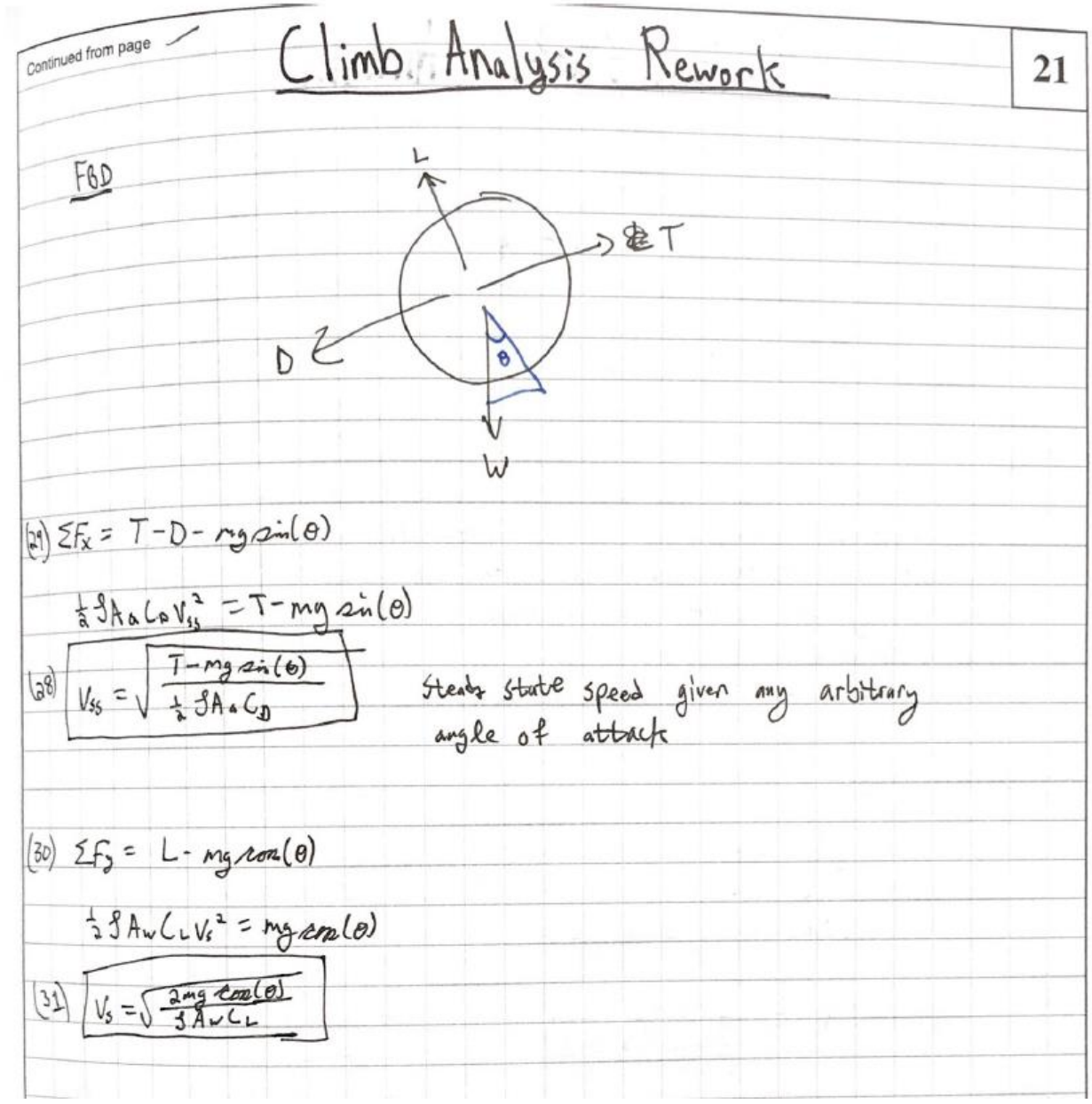

Continued from page

# Climb Analysis Rework

21

FBD

L

T

D

θ

W

(29) $\Sigma F_x = T - D - mg\sin(\theta)$

$\frac{1}{2}\rho A_a C_D V_{ss}^2 = T - mg\sin(\theta)$

(28) $V_{ss} = \sqrt{\frac{T - mg\sin(\theta)}{\frac{1}{2}\rho A_a C_D}}$

Steady state speed given any arbitrary angle of attack

(30) $\Sigma F_y = L - mg\cos(\theta)$

$\frac{1}{2}\rho A_w C_L V_s^2 = mg\cos(\theta)$

(31) $V_s = \sqrt{\frac{2mg\cos(\theta)}{\rho A_w C_L}}$

## Appendix H: Takeoff Analysis

Continued from page

# Takeoff Analysis

19

### Takeoff Procedure

Aircraft will accelerate along ground until it reaches 120% of the stall speed. When this occurs, the pilot will order the elevators up in order to generate an upward moment and pitch the aircraft's nose up into the air.

### Free Body Diagram

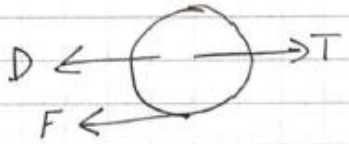


T = Thrust
D = Drag
F = Friction

$\Sigma F_x = T - D - F$

(3) $V_s^2 = \cancel{V_0^2}^{0} + 2aX_{to}$ (starts from rest)

$X_{to} = \frac{V_s^2}{2a}$

Substitutions: (1) $F_{net} = ma \rightarrow a = \frac{F_{net}}{m}$

$F_{net} = T - D - F$

(9) $\rightarrow V_s = \sqrt{\frac{2mg}{\rho A_w C_L}}$

$F = \mu_s mg$

$\rightarrow a = \frac{T - D - \mu_s mg}{m}$

$X_{to} = \frac{\left(\sqrt{\frac{2mg}{\rho A_w C_L}}\right)^2}{2\left(\frac{T - D - \mu_s mg}{m}\right)}$

$X_{to} = \frac{2m^2 g}{2(\rho A_w C_L)(T - D - \mu_s mg)}$

$X_{to} = \frac{m^2 g}{(\rho A_w C_L)(T - D - \mu_s mg)}$ $\rightarrow X_{TO} = FS \cdot X_{to}$ s.t. $FS = 1.20$

(24) $\boxed{X_{TO} = \frac{(1.20)(m^2 g)}{(\rho A_w C_L)(T - D - \mu_s mg)}}$

Con't

Continued to page 20

Continued from page 19

Recall (24) $X_{TO} = \frac{(FS)m^2g}{(\rho A_w C_L)(T - D - \mu_s mg)}$

St. (6) $D = \frac{1}{2}\rho A_a C_D V^2$

and (9) $V = \sqrt{\frac{2mg}{\rho A_w C_L}}$

$\therefore D = \frac{1}{2}\rho A_a C_D \frac{2mg}{\rho A_w C_L}$

$D = \frac{A_a C_D mg}{A_w C_L}$

(25) $\boxed{X_{TO} = \frac{(FS)m^2g}{(\rho A_w C_L)(T - \frac{A_a C_D mg}{A_w C_L} - \mu_s mg)}}$ This fails because Drag is constantly changing with respect to velocity.

During takeoff, three net forces act on the aircraft:

- Thrust
- Drag
- Friction (sliding)

At stall speed,

$D = 0.2121$ (via MATLAB)

$F = 5.8860$

$D/F = 3.6033\%$

$\therefore$ Drag during takeoff can be considered negligible!

(26) $\boxed{X_{TO\_ND} = \frac{(FS)m^2g}{(\rho A_w C_L)(T - \mu_s mg)}}$ Neglecting Drag

Because stall speed is squared in (3), it is the most important factor to control. It is currently very high and is causing the aircraft to need a very large runway for takeoff. A launched takeoff may be required if total mass cannot be decreased or wing area increased.

Continued to page

SIGNATURE Matthew S. Clyne DATE 12/19/18

DISCLOSED TO AND UNDERSTOOD BY CB DATE 12/21/18

PROPRIETARY INFORMATION

## Appendix I: Bill of Material and Technical Specifications of Components

| Bill of Material | | | | | | | |
|---|---|---|---|---|---|---|---|
| Log | Item | Cost | Purchaser | Times Purchased | Total Cost | Unit Ratio | Unit Cost |
| 1 | Motor, T-Motors, U5 KV400 | $119.99 | Chapman | 1 | $119.99 | 1 | $ 119.99 |
| 2 | Propeller. T-Motors,14*4.8 CF | $ 48.90 | Chapman | 1 | $ 48.90 | 0.5 | $ 24.45 |
| 3 | Freewing 17g Digital Metal Gear Servo with 550mm (22") Lead | $ 9.99 | Barr | 4 | $ 39.96 | 1 | $ 39.96 |
| 4 | ZTW Mantis 45A ESC with 5A SBEC | $ 28.90 | Barr | 1 | $ 28.90 | 1 | $ 28.90 |
| 5 | AS3X Programming Cable - USB Interface | $ 16.98 | Barr | 1 | $ 16.98 | 1 | $ 16.98 |
| 6 | Admiral 300mm (12") Servo Y Extension Cable | $ 1.09 | Barr | 1 | $ 1.09 | 1 | $ 1.09 |
| 7 | Admiral 450mm (18") Servo Extension Cable | $ 0.99 | Barr | 2 | $ 1.98 | 1 | $ 1.98 |
| 8 | Dubro Nylon T-Style Control Horns (2 Pack) | $ 1.08 | Barr | 3 | $ 3.24 | 1 | $ 3.24 |
| 9 | Dubro 2-56 305mm / 12" Threaded Rod (6 Pack) | $ 3.49 | Barr | 1 | $ 3.49 | 1 | $ 3.49 |
| 10 | Dubro 22.86mm / 0.90" Nylon Kwik-Link Standard Clevis (2) | $ 0.98 | Barr | 3 | $ 2.94 | 1 | $ 2.94 |
| 11 | ZIPPY Compact 5800mAh 6S 25C Lipo Pack With XT90 | $ 71.53 | Barr | 1 | $ 71.53 | 1 | $ 71.53 |
| 12 | Admiral RX600Sp-6-Channel DSMX Receiver | $ 29.99 | Knutty | 1 | $ 29.99 | 1 | $ 29.99 |
| 13 | Spektrum DXe 6-Channel Transmitter | $ 69.99 | Knutty | 1 | $ 69.99 | 0 | $ - |
| 14 | SkyC 86AC V2 50W 6Cell (6S)AC/DC Lipo Battery Charger | $ 59.99 | Knutty | 1 | $ 59.99 | 0 | $ - |
| 15 | Carbon Fiber Tubes 24 in OD 0.21 | $ 6.99 | Knutty | 2 | $ 13.98 | 1 | $ 13.98 |
| 16 | Carbon Fiber Tubes 24 in OD 0.18 | $ 6.99 | Knutty | 1 | $ 6.99 | 1 | $ 6.99 |
| 17 | Carbon Fiber Tubes 40 in OD 0.21 | $ 8.99 | Knutty | 1 | $ 8.99 | 1 | $ 8.99 |
| 18 | Arduino Nano | $ 13.86 | Chapman | 1 | $ 13.86 | 0.3333333 | $ 4.62 |
| 19 | Accelerometer | $ 10.99 | Chapman | 1 | $ 10.99 | 1 | $ 10.99 |
| 20 | Temperature Sensor | $ 10.49 | Chapman | 1 | $ 10.49 | 0.2 | $ 2.10 |
| 21 | Current Sensor | $ 8.66 | Chapman | 1 | $ 8.66 | 1 | $ 8.66 |
| 22 | Voltage Sensor | $ 9.99 | Chapman | 1 | $ 9.99 | 0.2 | $ 2.00 |
| 23 | Du-BRO 200TW 2" Diameter Wheel | $ 4.86 | Knutty | 1 | $ 4.86 | 1 | $ 4.86 |
| 24 | SIG SH146 Flat Head Wood Screws | $ 1.99 | Knutty | 4 | $ 7.96 | 0.025 | $ 0.20 |
| 25 | DU-BRO 893 Socket HEad Servo Mounting Screws (24 pack) | $ 3.82 | Knutty | 4 | $ 15.28 | 0.0416 | $ 0.64 |
| 26 | DU-BRO 381 No. 2 x 1/2" Socket Head Sheet Metal Screws | $ 2.25 | Knutty | 4 | $ 9.00 | 0.025 | $ 0.23 |
| 27 | DU-BRO 246 1-1/4" Long x 1/8" Diam Spring Steel Axel Shaft | $ 6.39 | Knutty | 1 | $ 6.39 | 0.5 | $ 3.20 |
| 28 | DU-BRO 140 5/32" Plated Brass Dura-Collars | $ 2.15 | Knutty | 1 | $ 2.15 | 0.25 | $ 0.54 |
| 29 | DU-BRO 139 1/8" Plated Brass Dura-Collars | $ 2.15 | Knutty | 1 | $ 2.15 | 0.25 | $ 0.54 |
| 30 | Shaft | $ 6.39 | Knutty | 1 | $ 6.39 | 0.5 | $ 3.20 |
| 31 | DU-BRO HEAVY DUTY HINGES | $ 7.60 | Knutty | 2 | $ 15.20 | 0.1 | $ 1.52 |
| 32 | bsi AT 5 Minute Epoxy - Small | $ 7.99 | Knutty | 1 | $ 7.99 | 1 | $ 7.99 |
| 33 | Servo Motor (Custom Item) | $ 15.99 | Knutty | 1 | $ 15.99 | 1 | $ 15.99 |
| 34 | Hatchbox PLA 3D Printing Filament | $ 19.99 | Knutty | 4 | $ 79.96 | 0.25 | $ 19.99 |
| 35 | Carbon Fiber Tubes 8mm x 6mm x 1000mm | $ 24.99 | Knutty | 1 | $ 24.99 | 0.25 | $ 6.25 |
| 36 | Carbon Fiber Flat Bar 4mm x 20mm x 1000mm | $ 29.99 | Knutty | 1 | $ 29.99 | 0.5 | $ 15.00 |
| 37 | HiLetgo 5 pcs Micro SD Card Adater Teader Midule | $ 6.99 | Knutty | 1 | $ 6.99 | 1 | $ 6.99 |
| 38 | SanDisk 32 GB Mobile MicroSDHC Class 4 Flash Memory Card | $ 6.99 | Knutty | 1 | $ 6.99 | 1 | $ 6.99 |
| 39 | Female XT60 to XT90 / XT-90 Male Adapter | $ 3.10 | Barr | 1 | $ 3.10 | 0.5 | $ 1.55 |
| | | | | | | | |
| | | | | TOTALS | $828.30 | | $ 498.55 |

# Bill of Material

| Log | Item | Cost | Purchaser | Times Purchased | Total Cost | Unit Ratio | Unit Cost | Link |
|---|---|---|---|---|---|---|---|---|
| 1 | Motor, T-Motors, U5 KV400 | $119.99 | Chapman | 1 | $119.99 | 1 | $ 119.99 | http://store-en.tmotor.com/goods.php?id=318 |
| 2 | Propeller. T-Motors,14*4.8 CF | $ 48.90 | Chapman | 1 | $ 48.90 | 0.5 | $ 24.45 | https://www.robotshop.com/en/t-motor-14-48-carbon-fiber-propeller-pair.html |
| 3 | Freewing 17g Digital Metal Gear Servo with 550mm (22") Lead | $ 9.99 | Barr | 4 | $ 39.96 | 1 | $ 39.96 | https://www.motionrc.com/products/freewing-17g-digital-metal-gear-servo-with-550mm-lead-md31172-550?variant=30792291276 |
| 4 | ZTW Mantis 45A ESC with 5A SBEC | $ 28.90 | Barr | 1 | $ 28.90 | 1 | $ 28.90 | https://www.motionrc.com/products/ztw-mantis-45a-esc-with-5a-sbec?variant=19068822918 |
| 5 | AS3X Programming Cable - USB Interface | $ 16.98 | Barr | 1 | $ 16.98 | 1 | $ 16.98 | https://www.motionrc.com/products/as3x-programming-cable-usb-interface?variant=19069433926 |
| 6 | Admiral 300mm (12") Servo Y Extension Cable | $ 1.09 | Barr | 1 | $ 1.09 | 1 | $ 1.09 | https://www.motionrc.com/products/300mm-12-servo-y-extension-cable?variant=19052388550 |
| 7 | Admiral 450mm (18") Servo Extension Cable | $ 0.99 | Barr | 2 | $ 1.98 | 1 | $ 1.98 | https://www.motionrc.com/products/450mm-18-servo-extension-cable?variant=19052216774 |
| 8 | Dubro Nylon T-Style Control Horns (2 Pack) | $ 1.08 | Barr | 3 | $ 3.24 | 1 | $ 3.24 | https://www.motionrc.com/products/dubro-nylon-t-style-control-horns-2-pack?variant=19046976070 |
| 9 | Dubro 2-56 305mm / 12" Threaded Rod (6 Pack) | $ 3.49 | Barr | 1 | $ 3.49 | 1 | $ 3.49 | https://www.motionrc.com/products/dubro-2-56-threaded-rod-12-305mm6-pack?variant=198136463385 |
| 10 | Dubro 22.86mm / 0.90" Nylon Kwik-Link Standard Clevis (2) | $ 0.98 | Barr | 3 | $ 2.94 | 1 | $ 2.94 | https://www.motionrc.com/products/dubro-nylon-kwik-link-standard-clevis-2?variant=19046473158 |
| 11 | ZIPPY Compact 5800mAh 6S 25C Lipo Pack With XT90 | $ 71.53 | Barr | 1 | $ 71.53 | 1 | $ 71.53 | https://hobbyking.com/en_us/zippy-compact-5800mah-6s-25c-lipo-pack-xt90.html |
| 12 | Admiral RX600Sp-6-Channel DSMX Receiver | $ 29.99 | Knutty | 1 | $ 29.99 | 1 | $ 29.99 | https://www.motionrc.com/products/admiral-rx600sp-6-channel-dsmx-compatible-receiver-with-6-axis-stabilizer |
| 13 | Spektrum DXe 6-Channel Transmitter | $ 69.99 | Knutty | 1 | $ 69.99 | 0 | $ - | https://www.motionrc.com/products/spektrum-dxe-6-channel-transmitter |
| 14 | SkyC 86AC V2 50W 6Cell (6S)AC/DC Lipo Battery Charger | $ 59.99 | Knutty | 1 | $ 59.99 | 0 | $ - | https://www.motionrc.com/collections/battery-chargers/products/skyrc-b6ac-v2-ac-dc-charger |
| 15 | Carbon Fiber Tubes 24 in OD 0.21 | $ 6.99 | Knutty | 2 | $ 13.98 | 1 | $ 13.98 | https://www.hobbytown.com/midwest-carbon-fiber-tube-24-.210-od-mid5724/p50678?gclid=EAIaIQobChMIjsiMwdPm4AIVDo1pCh0ZIAzfEAkYAiABEgKGsfD_BwE |
| 16 | Carbon Fiber Tubes 24 in OD 0.18 | $ 6.99 | Knutty | 1 | $ 6.99 | 1 | $ 6.99 | https://www.hobbytown.com/midwest-carbon-fiber-tube-24-.188-od-mid5722/p50676?gclid=EAIaIQobChMI3fqJrNPm4AIVgrbACh0_ug9REAkYASABEgLSBfD_BwE |
| 17 | Carbon Fiber Tubes 40 in OD 0.21 | $ 8.99 | Knutty | 1 | $ 8.99 | 1 | $ 8.99 | https://www.hobbyzone.com/mid5822.html?utm_source=Google&utm_campaign=Google+Shopping&gclid=EAIaIQobChMI9NWb0dPm4AIVgRlpCh3z3gDmEAkYBiABEgJei_D_BwE |
| 18 | Arduino Nano | $ 13.86 | Chapman | 1 | $ 13.86 | 0.3333333 | $ 4.62 | https://smile.amazon.com/gp/product/B0713XK923/ref=ppx_yo_dt_b_asin_title_o02_s00?ie=UTF8&psc=1 |
| 19 | Accelerometer | $ 10.99 | Chapman | 1 | $ 10.99 | 1 | $ 10.99 | https://smile.amazon.com/gp/product/B0151GI5VI/ref=ppx_yo_dt_b_asin_title_o02_s00?ie=UTF8&psc=1 |
| 20 | Temperature Sensor | $ 10.49 | Chapman | 1 | $ 10.49 | 0.2 | $ 2.10 | https://smile.amazon.com/gp/product/B01DKC2GQ0/ref=ppx_yo_dt_b_asin_title_o02_s01?ie=UTF8&psc=1 |
| 21 | Current Sensor | $ 8.66 | Chapman | 1 | $ 8.66 | 1 | $ 8.66 | https://smile.amazon.com/gp/product/B079P4LVPV/ref=ppx_yo_dt_b_asin_title_o02_s01?ie=UTF8&psc=1 |
| 22 | Voltage Sensor | $ 9.99 | Chapman | 1 | $ 9.99 | 0.2 | $ 2.00 | https://smile.amazon.com/gp/product/B07L81QJ75/ref=ppx_yo_dt_b_asin_title_o02_s01?ie=UTF8&psc=1 |
| 23 | Du-BRO 200TW 2" Diameter Wheel | $ 4.86 | Knutty | 1 | $ 4.86 | 1 | $ 4.86 | https://www.motionrc.com/products/dubro-2-dia-treaded-lightweight-wheel-2-pack |
| 24 | SIG SH146 Flat Head Wood Screws | $ 1.99 | Knutty | 4 | $ 7.96 | 0.025 | $ 0.20 | http://brodak.com/sig-wood-screw-flat-head-2-x-3-8.html |
| 25 | DU-BRO 893 Socket HEad Servo Mounting Screws (24 pack) | $ 3.82 | Knutty | 4 | $ 15.28 | 0.0416 | $ 0.64 | https://www.motionrc.com/products/dubro-socket-head-servo-mounting-screws-2x7-1624-pieces |
| 26 | DU-BRO 381 No. 2 x 1/2" Socket Head Sheet Metal Screws | $ 2.25 | Knutty | 4 | $ 9.00 | 0.025 | $ 0.23 | https://www.motionrc.com/products/dubro-2-x-1-2-socket-head-sheet-metal-screws-8-pack |
| 27 | DU-BRO 246 1-1/4" Long x 1/8" Diam Spring Steel Axel Shaft | $ 6.39 | Knutty | 1 | $ 6.39 | 0.5 | $ 3.20 | https://www.motionrc.com/products/dubro-1-8-x-1-1-4-spring-steel-axle-shaft-with-nylon-insert-lo |
| 28 | DU-BRO 140 5/32" Plated Brass Dura-Collars | $ 2.15 | Knutty | 1 | $ 2.15 | 0.25 | $ 0.54 | https://www.motionrc.com/products/dubro-dura-collars-5-32-4-pack |
| 29 | DU-BRO 139 1/8" Plated Brass Dura-Collars | $ 2.15 | Knutty | 1 | $ 2.15 | 0.25 | $ 0.54 | https://www.motionrc.com/products/dubro-dura-collars-1-8-4-pack |
| 30 | Shaft | $ 6.39 | Knutty | 1 | $ 6.39 | 0.5 | $ 3.20 | https://www.motionrc.com/products/dubro-5-32-x-2-spring-steel-axle-shaft-with-nylon-insert-lock |
| 31 | DU-BRO HEAVY DUTY HINGES | $ 7.60 | Knutty | 2 | $ 15.20 | 0.1 | $ 1.52 | https://www.motionrc.com/products/dubro-heavy-duty-nylon-hinges-15-pack |
| 32 | bsi AT 5 Minute Epoxy - Small | $ 7.99 | Knutty | 1 | $ 7.99 | 1 | $ 7.99 | https://www.amazon.com/BSI-BSI-202-Quick-Cure-Epoxy-Smith/dp/B0002BBV46 |
| 33 | Servo Motor (Custom Item) | $ 15.99 | Knutty | 1 | $ 15.99 | 1 | $ 15.99 | |
| 34 | Hatchbox PLA 3D Printing Filament | $ 19.99 | Knutty | 4 | $ 79.96 | 0.25 | $ 19.99 | https://www.amazon.com/HATCHBOX-Red-PLA-Printer-Filament/dp/B00J0GO8I0/ref=sr_1_7?keywords=hatchbox+pla&qid=1554743050&s=hi&sr=1-7-catcorr |
| 35 | Carbon Fiber Tubes 8mm x 6mm x 1000mm | $ 24.99 | Knutty | 1 | $ 24.99 | 0.25 | $ 6.25 | https://www.amazon.com/gp/product/B07KWHF22P/ref=ppx_yo_dt_b_asin_title_o01_s00?ie=UTF8&psc=1 |
| 36 | Carbon Fiber Flat Bar 4mm x 20mm x 1000mm | $ 29.99 | Knutty | 1 | $ 29.99 | 0.5 | $ 15.00 | https://www.amazon.com/gp/product/B07KXK2WPJ/ref=ppx_yo_dt_b_asin_title_o01_s00?ie=UTF8&psc=1 |
| 37 | HiLetgo 5 pcs Micro SD Card Adater Teader Midule | $ 6.99 | Knutty | 1 | $ 6.99 | 1 | $ 6.99 | https://www.amazon.com/gp/product/B07BJ2P6X6/ref=ppx_yo_dt_b_asin_title_o00_s00?ie=UTF8&psc=1 |
| 38 | SanDisk 32 GB Mobile MicroSDHC Class 4 Flash Memory Card | $ 6.99 | Knutty | 1 | $ 6.99 | 1 | $ 6.99 | https://www.amazon.com/gp/product/B003HIWHN0/ref=ppx_yo_dt_b_asin_title_o00_s00?ie=UTF8&psc=1 |
| 39 | Female XT60 to XT90 / XT-90 Male Adapter | $ 3.10 | Barr | 1 | $ 3.10 | 0.5 | $ 1.55 | https://www.ebay.com/itm/153133083035 |
| | | | | | | | | |
| | | | | TOTALS | $828.30 | | $ 498.55 | |

ESC

**PRODUCT SPECIFICATIONS:**

| | |
|---|---|
| Length | 57mm / 2.24in |
| Width | 31mm / 1.22in |
| Height | 12mm / 0.47in |
| Weight | 56g |
| MAX Output | Continuous Current 45A |
| Burst Output | 65A (10s) |
| Battery | 2-6Lipo/5-18NC |
| BEC Output | 5V 5.5V 6V Adjustable/5A |
| Power Connector | XT60 Connector |
| Motor Connector | 3.5mm bullets |

Battery

| | |
|---|---|
| SKU | 9067000302-0 |
| Shipping Weight | 894.0000 |
| Packaging Width | 54.00 |
| Capacity (mAh) | 5800.00 |
| Length-A(mm) | 157.00 |
| Width-C(mm) | 45.00 |

| | |
|---|---|
| Brand | Zippy |
| Packaging Length | 188.40 |
| Packaging Height | 63.60 |
| Discharge(c) | 25.00 |
| Height-B(mm) | 53.00 |

Receiver

PRODUCT SPECIFICATIONS:

| | |
|---|---|
| Number of Channels | 6 |
| Modulation / Protocol | DSMX™ Compatible |
| Band | 2.4GHz |
| Range | Full |
| Telemetry | No |
| Integrated Gyro | 6-Axis |
| Voltage Range | 3.45-8.4V |
| Antenna | Dual Diversity |
| Dimensions (L x W x H) | 37.4 x 27.6 x 9mm |
| Weight | 7g |

Transmitter

PRODUCT SPECIFICATIONS:

| | |
|---|---|
| Number of Channels | 6 |
| Modulation / Protocol | DSMX |
| Band | 2.4Ghz |
| Mode(s) | Mode 1-4 (Default Mode 2) |
| Model Memory | Unlimited Aircraft (via Mobile App) |
| Display | None |
| Rotary Knobs | None |
| 2-Position Switches | 1 |
| 3-Position Switches | 1 |
| Slider Switches | None |
| Momentary Switches | 1 |
| Gimbals | Bushing |
| Telemetry | No |
| Voice Alerts | No |
| Memory Card Support | No |
| Data Port | No |
| Upgradeable Firmware | No |
| Trainer System | No |
| Dual Rate / Expo | No |
| Throttle Cut | No |
| Servo Speed Adjustment | No |
| Battery | 4 AA (Included) |

## Accelerometer

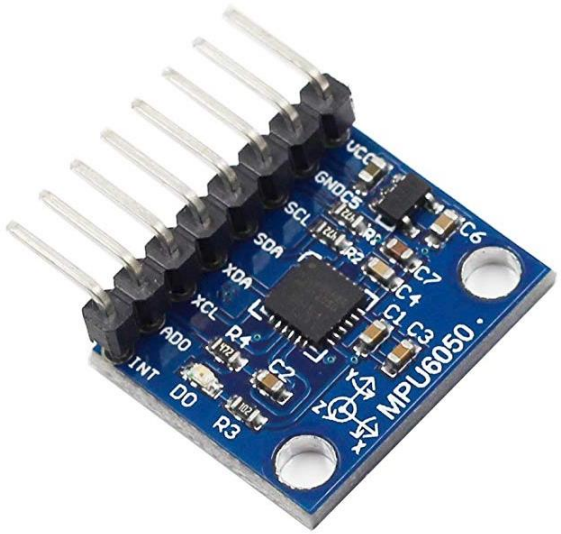


SunFounder MPU6050 Module for Arduino and Raspberry Pi, 3-axis Gyroscope and 3-axis Accelerator

by SunFounder

6 customer reviews

Amazon's Choice for "mpu6050"

Price: $10.99 prime

FREE One-Day Pickup. Details

Pay ~~$10.99~~ $0.00 after using available Discover Cashback Bonus®.

Eligible for amazonsmile donation.

- Integrates 3-axis gyroscope and 3-axis accelerator, including the hardware accelerator engine for devices connected to the second I2C port, like another accelerator of other brands, magnetometer, or Digital Motion Processor (DMP) of other sensors
- With three 16-bit analog-to-digital converters (ADCs) for digitizing the gyroscope outputs and another three ones for digitizing the accelerometer outputs
- Supports the I2C serial interface and has a separate VLOGIC reference pin
- User-programmable gyroscope, with a full-scale range of ±250, ±500, ±1000, and ±2000°/sec (dps) and a user-programmable accelerometer with a full-scale range of ±2g, ±4g, ±8g, and ±16g
- Working voltage: 3.3v-5v; PCB size: 1.65 x 2.0 cm

Compare with similar items

New (1) from $10.99 prime

Report incorrect product information.

Save on Quality Cables by AmazonBasics

## Temperature Sensor

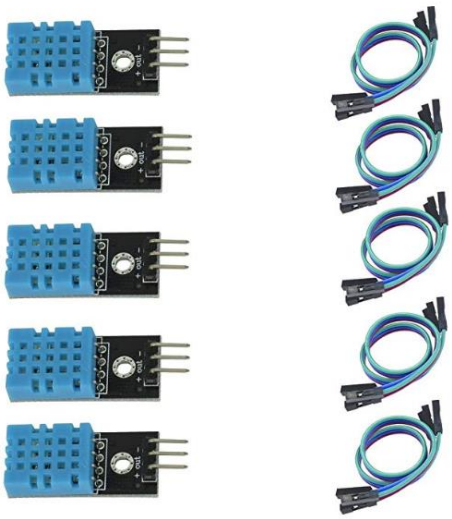

HiLetgo

HiLetgo 5pcs DHT11 Temperature and Humidity Sensor Module for Arduino Raspberry Pi 2 3

29 customer reviews

Amazon's Choice for "dht11"

Price: $10.49 prime

FREE One-Day Pickup. Details

FREE Returns

Eligible for amazonsmile donation.

- DHT11 digital temperature and humidity sensor is a digital signal output with a calibrated temperature and humidity combined sensor.
- It uses a dedicated digital modules and acquisition of temperature and humidity sensor technology to ensure that products with high reliability and excellent long term stability.
- Sensor consists of a resistive element and a sense of wet NTC temperature measurement devices, and with a high-performance 8-bit microcontroller connected.
- The product has excellent quality, fast response, anti-interference ability, high cost and other advantages.
- The single-wire wiring scheme makes it easy to be integrated to other applications.And the simple communication protocol greatly reduces the programming effort required.

New (1) from $10.49 prime

Report incorrect product information.

Save on AmazonBasics and SupplyMaster Safety Gear

SupplyMaster Disposable Exam Nitrile

AmazonBasics Blue Light Blocking

AmazonBasics Noise Reduction

## Current Sensors


FTCBlock 3pcs ACS712 Current Sensor 30A Range Analogue AC/DC for Arduino Ras PI

by FTCBlock

1 customer review

Price: $8.66 ($2.89 / Item) prime

FREE One-Day Pickup. Details

Eligible for amazonsmile donation.

Size: **30A**

| 5A | 20A | 30A |
|---|---|---|
| $8.66 ($2.89 / Item) prime | $8.66 ($2.89 / Item) prime | **$8.66 ($2.89 / Item)** prime |

- Current sensor chip: ACS712ELC-30A
- Pin 5V power supply, on-board power indicator
- The module can measure the positive and negative 20 amps, corresponding to the analog output 100mV / A
- There is no the detection current through, the output voltage is VCC / 2
- The PCB board size: 31 (mm) x13 (mm)

## Voltage Sensor

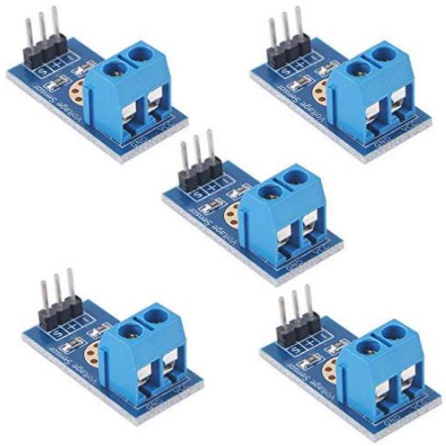

DC0-25V Voltage Tester Sensor Terminal for Arduino Raspberry Pi(Pack of 5pcs), Measure up to 25V

by Stemedu

Be the first to review this item

Price: $9.99 prime

Eligible for amazonsmile donation.

- Document link: https://www.instructables.com/id/Arduino-Voltage-Sensor-0-25V/
- Voltage input range: DC0-25V
- Output interface: "+" 5V/3.3V, "-" GND, "S" Arduino AD pins
- What you will get: 5PCS DC0-25V Voltage Tester Sensor
- Warranty: Life time warranty, any question please feel free to contact.How to email us? Please click "Stemedu" and click "Ask a question" to email us

**Specifications for this item**

| | |
|---|---|
| Brand Name | Stemedu |
| Part Number | ST0430X5 |

See more product details

**New** (1) from $9.99 prime

Report incorrect product information.

**Download Alexa for your Windows 10 PC for free**

Experience the convenience of Alexa, now on your PC. Download now

## Expendable Drone Electrical Component Specifications

| Brushless Motor | |
|---|---|
| T-Motor U5 400KV | |
| Weight | 195g |
| Dimensions | ø42.5x37.5mm |
| No. of Cells | 3-8S |
| Connector | 3.5mm bullets |
| Internal Resistance | 116mΩ |
| Max Continuous Power | 850W |
| Idle Current | 0.3A |
| Max Continuous Current | 30A |
| Current @ 50% Throttle | 3.4A |
| Current @ 100% Throttle | 13.7A |

| Battery | |
|---|---|
| Zippy Compact Lipo Pack | |
| Weight | 745g |
| Dimensions (LxWxH) | 157x45x53mm |
| No. of Cells | 6 Cell |
| Connector | XT90 |
| Nominal Voltage | 22.2V |
| Capacity | 5800mAh |
| Constant Discharge Rate | 25C |
| Burst Discharge Rate | 50C |

| Electronic Speed Controller (ESC) | |
|---|---|
| ZTW Mantis 45A ESC w/ 5A BEC | |
| Weight | 56g |
| Dimensions (LxWxH) | 57x31x12mm |
| No. of Cells | 2-6S |
| Connector (to motor) | 3.5mm bullets |
| Connector (to battery) | XT60 |
| Max Continuous Output | 45A |
| Max Burst Output | 65A (10s) |
| BEC Voltage Output | 5-6V |
| BEC Current Output | 5A |

| Features |
|---|
| Programmable |
| Auto throttle shutdown w/ signal loss |
| Safety thermal overload protection |

| Reciever | |
|---|---|
| Admiral DSMX 6-Channel | |
| Weight | 7g |
| Dimensions (LxWxH) | 37.4x27.6x9mm |
| No. of Channels | 6 |
| Range | Full |
| Voltage | 3.45-8.4V |
| Gyro Capabilities | Yes |

| Control Surface Servos | |
|---|---|
| Freewing 17g Digital MG Servo | |
| Total Weight | 20g |
| Dimensions (LxWxH) | 28.5x13.5x30mm |
| Lead Length | 550mm |
| Gear Material | Metal |
| Operating Voltage Range | 4.8-6V |
| Current Draw Idle | 20mA |
| Current Draw Operating (No Loa | 120mA |
| Torque (4.8V) | 2.5 kg-cm |
| Torque (6V) | 3.0 kg-cm |
| Speed (4.8V) | 0.14 sec/60 deg |
| Speed (6V) | 0.13 sec/60 deg |

| Parachute Servo | |
|---|---|
| Tactic 9g TSX5 Micro Servo | |
| Total Weight | 9g |
| Dimensions (LxWxH) | 22.9x12x27.3mm |
| Gear Material | Plastic |
| Operating Voltage Range | 4.8-6V |
| Torque (4.8V) | 1.0 kg-cm |
| Torque (6V) | 1.0 kg-cm |
| Speed (4.8V) | 0.11 sec/60 deg |
| Speed (6V) | 0.09 sec/60 deg |

## Appendix J: Drawings and Images of the Aircraft

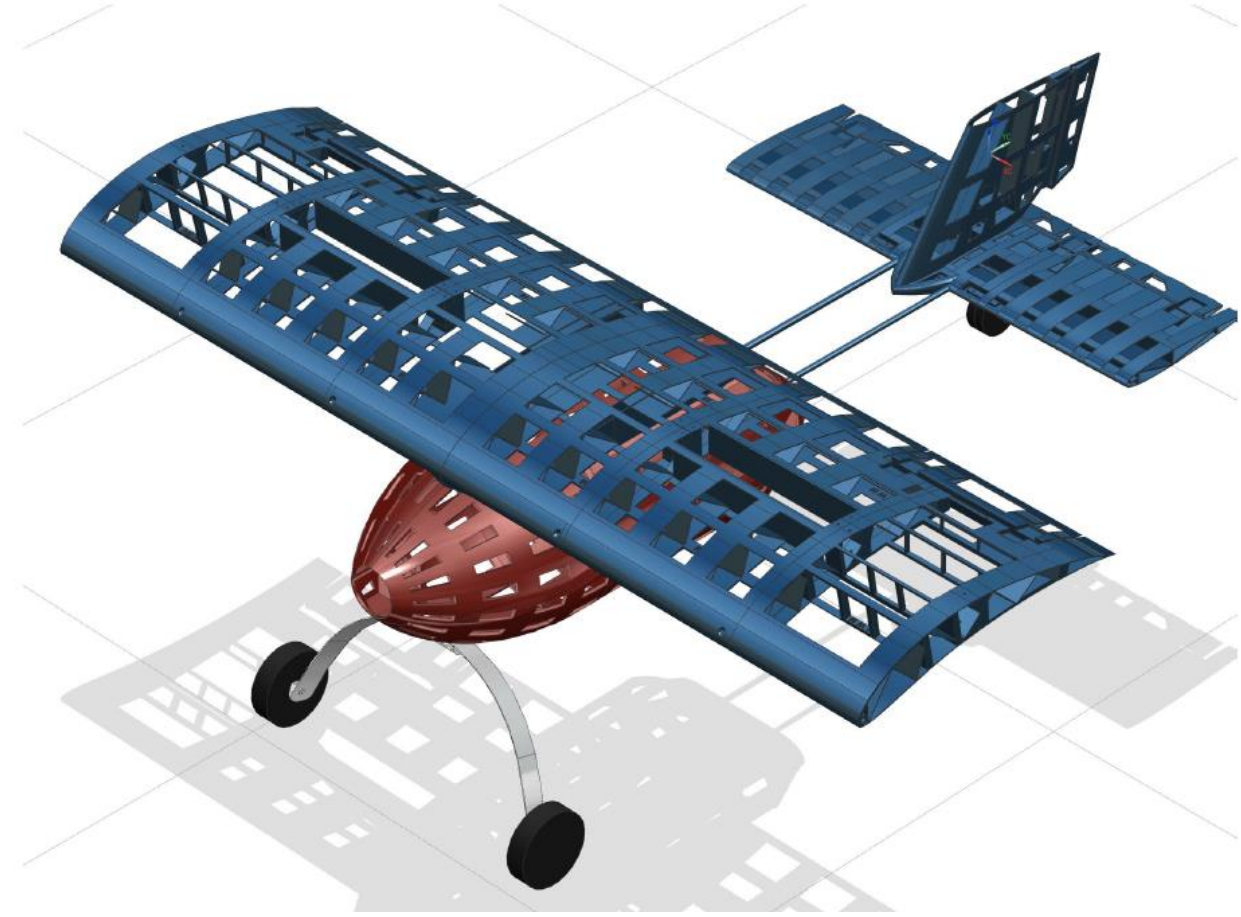

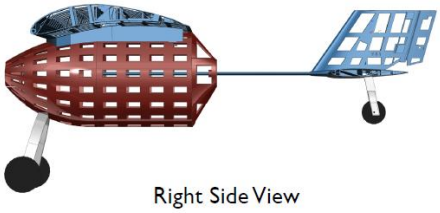

Right Side View

Front View

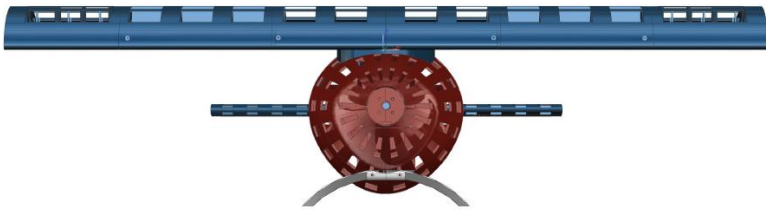

DRONE ASSEMBLY

Top View

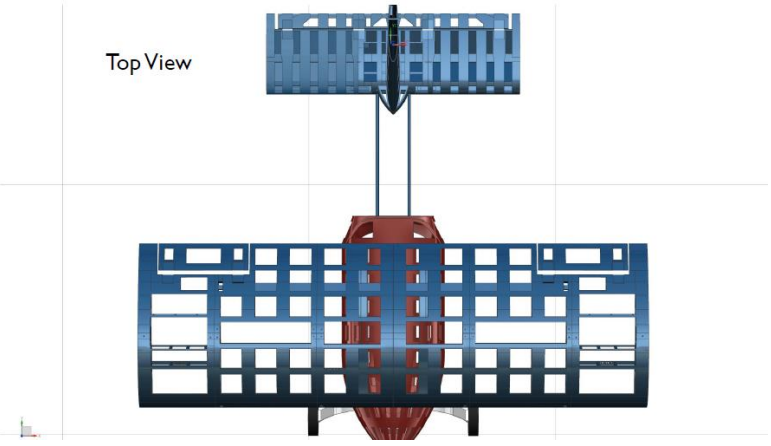

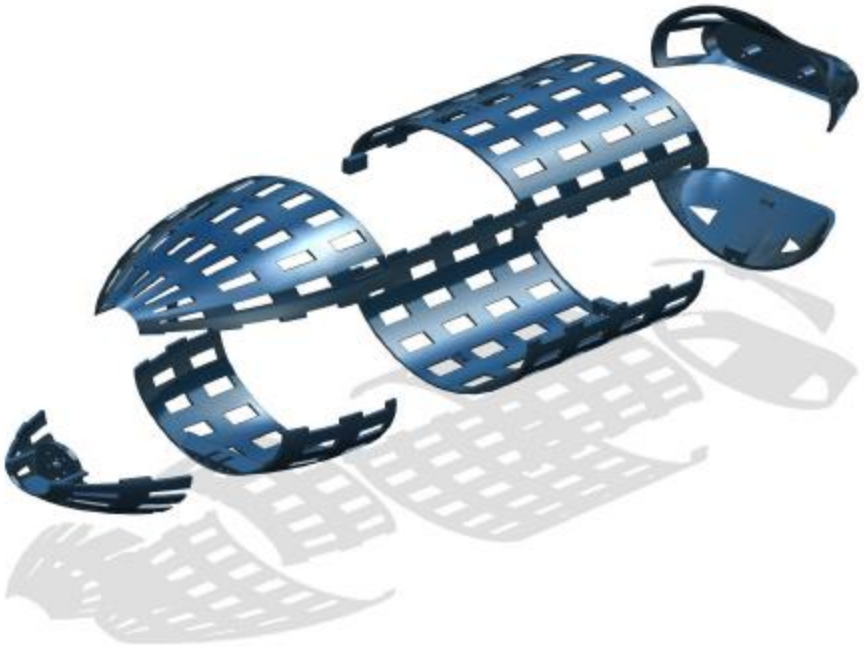

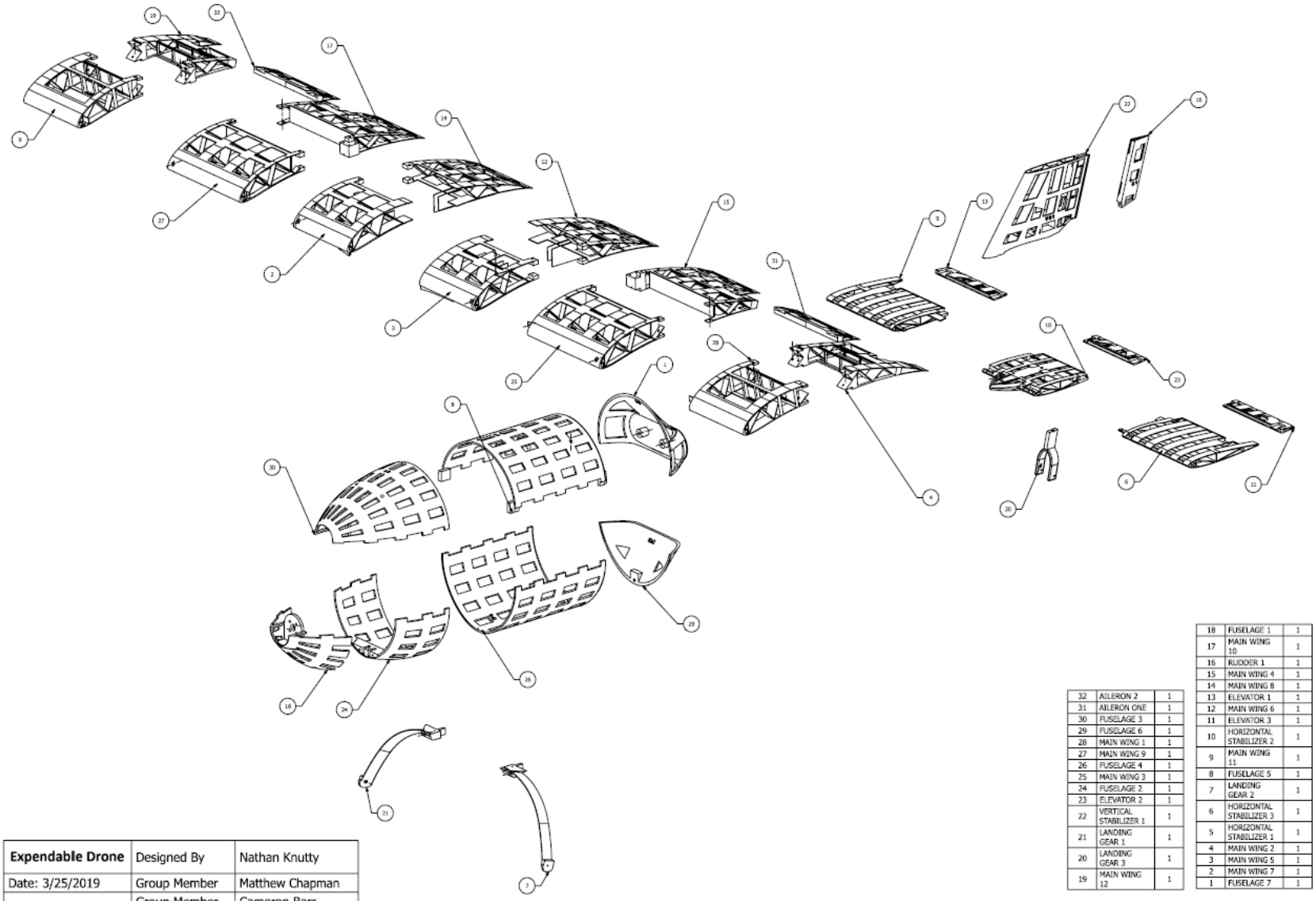

| | | |
|---|---|---|
| **Expendable Drone** | Designed By | Nathan Knutty |
| Date: 3/25/2019 | Group Member | Matthew Chapman |
| | Group Member | Cameron Barr |

| | | |
|---|---|---|
| 32 | AILERON 2 | 1 |
| 31 | AILERON ONE | 1 |
| 30 | FUSELAGE 3 | 1 |
| 29 | FUSELAGE 6 | 1 |
| 28 | MAIN WING 1 | 1 |
| 27 | MAIN WING 9 | 1 |
| 26 | FUSELAGE 4 | 1 |
| 25 | MAIN WING 3 | 1 |
| 24 | FUSELAGE 2 | 1 |
| 23 | ELEVATOR 2 | 1 |
| 22 | VERTICAL STABILIZER 1 | 1 |
| 21 | LANDING GEAR 1 | 1 |
| 20 | LANDING GEAR 3 | 1 |
| 19 | MAIN WING 12 | 1 |

| | | |
|---|---|---|
| 18 | FUSELAGE 1 | 1 |
| 17 | MAIN WING 10 | 1 |
| 16 | RUDDER 1 | 1 |
| 15 | MAIN WING 4 | 1 |
| 14 | MAIN WING 8 | 1 |
| 13 | ELEVATOR 1 | 1 |
| 12 | MAIN WING 6 | 1 |
| 11 | ELEVATOR 3 | 1 |
| 10 | HORIZONTAL STABILIZER 2 | 1 |
| 9 | MAIN WING 11 | 1 |
| 8 | FUSELAGE 5 | 1 |
| 7 | LANDING GEAR 2 | 1 |
| 6 | HORIZONTAL STABILIZER 3 | 1 |
| 5 | HORIZONTAL STABILIZER 1 | 1 |
| 4 | MAIN WING 2 | 1 |
| 3 | MAIN WING 5 | 1 |
| 2 | MAIN WING 7 | 1 |
| 1 | FUSELAGE 7 | 1 |

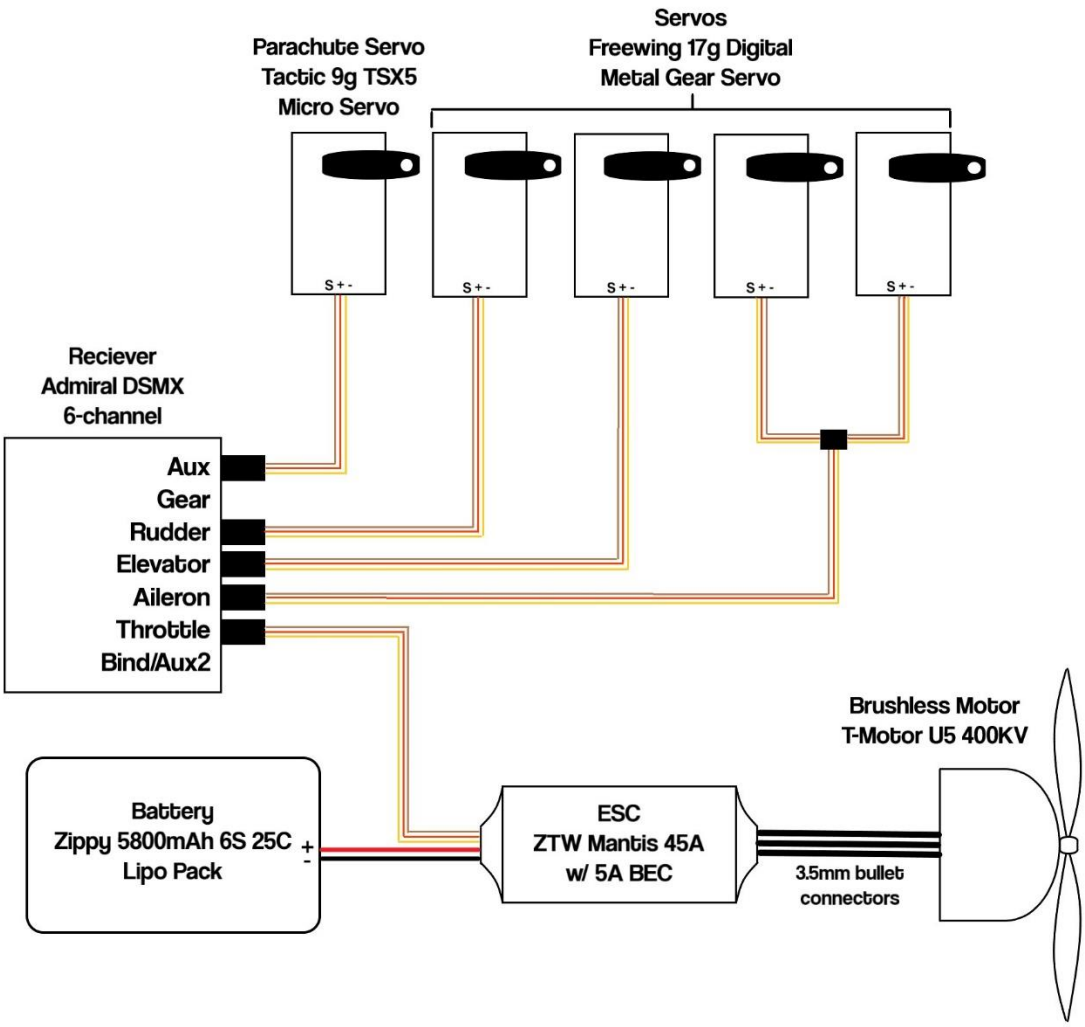
Servos
Freewing 17g Digital
Metal Gear Servo
Parachute Servo
Tactic 9g TSX5
Micro Servo
S + -
S + -
S + -
S + -
S + -
Reciever
Admiral DSMX
6-channel
Aux
Gear
Rudder
Elevator
Aileron
Throttle
Bind/Aux2
Brushless Motor
T-Motor U5 400KV
Battery
Zippy 5800mAh 6S 25C
Lipo Pack
+
-
ESC
ZTW Mantis 45A
w/ 5A BEC
3.5mm bullet
connectors

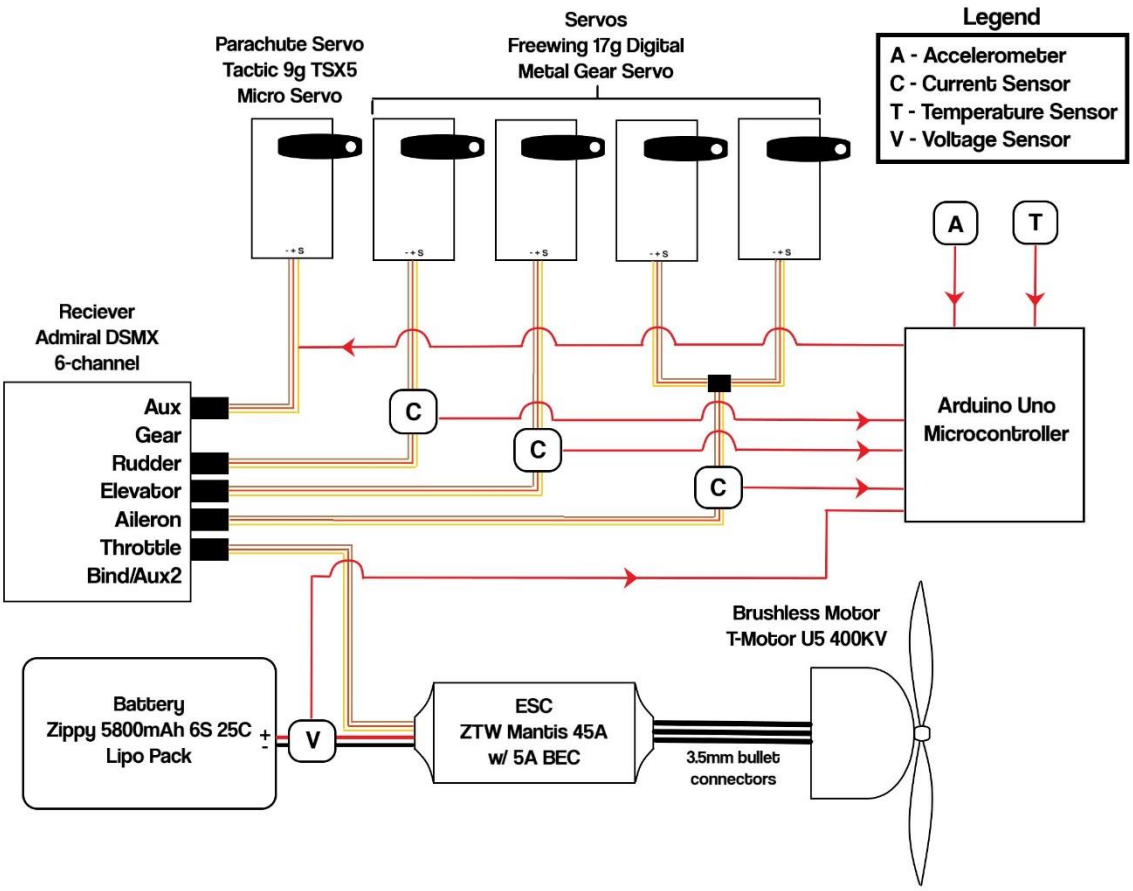
Parachute Servo
Tactic 9g TSX5
Micro Servo
Servos
Freewing 17g Digital
Metal Gear Servo
Legend
A - Accelerometer
C - Current Sensor
T - Temperature Sensor
V - Voltage Sensor
A
T
Reciever
Admiral DSMX
6-channel
Aux
Gear
Rudder
Elevator
Aileron
Throttle
Bind/Aux2
C
C
C
Arduino Uno
Microcontroller
Brushless Motor
T-Motor U5 400KV
Battery
Zippy 5800mAh 6S 25C
Lipo Pack
+
-
V
ESC
ZTW Mantis 45A
w/ 5A BEC
3.5mm bullet
connectors


GKZ 3373